6854–6869 *Nucleic Acids Research, 2022, Vol. 50, No. 12* *Published online 23 June 2022*
https://doi.org/10.1093/nar/gkac515

Host cell RecA activates a mobile element-encoded mutagenic DNA polymerase

Debika Ojha[1,†], Malgorzata M. Jaszczur[1,†], Adhirath Sikand[2], John P. McDonald[3], Andrew Robinson[4,5], Antoine M. van Oijen[4,5], Chi H. Mak[1,2,6], Fabien Pinaud[1,2,7], Michael M. Cox[8], Roger Woodgate[3] and Myron F. Goodman[1,2,*]

[1]Department of Biological Sciences, University of Southern California, Los Angeles, CA 90089, USA, [2]Department of Chemistry, University of Southern California, Los Angeles, Los Angeles, CA 90089, USA, [3]Laboratory of Genomic Integrity, National Institute of Child Health and Human Development, National Institutes of Health, Bethesda, MD 20892, USA, [4]Molecular Horizons Institute and School of Chemistry and Biomolecular Science, University of Wollongong, Wollongong, NSW 2522, Australia, [5]Illawarra Health and Medical Research Institute, Wollongong, NSW 2522, Australia, [6]Center of Applied Mathematical Sciences, University of Southern California, Los Angeles, CA 90089, USA, [7]Department of Physics and Astronomy, University of Southern California, Los Angeles, CA 90089, USA and [8]Department of Biochemistry, University of Wisconsin-Madison, Madison, WI 53706 Wisconsin, USA

Received February 25, 2022; Revised May 23, 2022; Editorial Decision May 28, 2022; Accepted May 31, 2022

ABSTRACT

Homologs of the mutagenic *Escherichia coli* DNA polymerase V (pol V) are encoded by numerous pathogens and mobile elements. We have used Rum pol (RumA′$_2$B), from the integrative conjugative element (ICE), R391, as a model mobile element-encoded polymerase (MEPol). The highly mutagenic Rum pol is transferred horizontally into a variety of recipient cells, including many pathogens. Moving between species, it is unclear if Rum pol can function on its own or requires activation by host factors. Here, we show that Rum pol biochemical activity requires the formation of a physical mutasomal complex, Rum Mut, containing RumA′$_2$B-RecA-ATP, with RecA being donated by each recipient bacteria. For R391, Rum Mut specific activities *in vitro* and mutagenesis rates *in vivo* depend on the phylogenetic distance of host-cell RecA from *E. coli* RecA. Rum pol is a highly conserved and effective mobile catalyst of rapid evolution, with the potential to generate a broad mutational landscape that could serve to ensure bacterial adaptation in antibiotic-rich environments leading to the establishment of antibiotic resistance.

INTRODUCTION

Pathogenic bacteria pose a major global threat through the precipitous emergence of multidrug resistant strains (https://www.cdc.gov/drugresistance/biggest-threats.html). Horizontal transfer of mobile genetic elements including R-plasmids, integrative-conjugative elements (ICEs) and chromosomal instabilities accompanied by high mutation rates are among the key factors driving antibiotic resistance (1–5). Recent data have provided new insights into sources of mutagenesis leading to drug resistance (6–12). Elevated mutagenesis accompanying the induction of the SOS stress response caused by exposure to antibiotics and, more generally, to a wide variety of exogeneous DNA damage, have been linked to development of bacterial antibiotic resistance (6,7,11,13–15). For example, exposure of clinical isolates of *Escherichia coli* to ciprofloxacin or zidovudine and *Acinetobacter baumannii* to UV or MMS resulted in the development of antibiotic resistance (15,16). There is a paucity of data documenting specific contributions of SOS-induced proteins, including pathogenic bacterial homologs of *E. coli* LexA repressor, RecA, and low-fidelity DNA polymerase V (pol V), toward the acquisition of drug resistance (6,7,15–18). Homologs of pol V have been identified in a variety of Gammaproteobacteria, many of which are pathogenic (15,19–23). In addition to homologs encoded chromosomally, many pol V homologs are found on mobile genetic elements that can be horizontally transferred between different bacterial species. We will refer to generic pol V homologs encoded on the chromosomes of pathogens by the term 'Pathogen Encoded Pols', abbreviated as PE-Pols. Homologous enzymes encoded by mobile elements, particularly integrative conjugative elements, or ICEs, will be referred to as Mobile Element encoded Pols (MEPols).

The biochemical and mutagenic properties of *E. coli* pol V, encoded by the *umuC* and *umuD* genes, have been in-

*To whom correspondence should be addressed. Tel: +1 213 740 5190; Fax: +1 213 821 1138; Email: mgoodman@usc.edu
†The authors wish it to be known that, in their opinion, the first two authors should be regarded as Joint First Authors.

vestigated extensively (24–34). Pol V is assembled as a heterotrimer composed of the SOS-induced UV-mutagenesis proteins UmuD′ and UmuC, pol V = UmuD′$_2$C (30,35). However, pol V is catalytically inactive and must be converted to an activated mutasome by the addition of a RecA subunit, pol V Mut = UmuD′$_2$C-RecA-ATP/ATPγS, to allow it to bind to and replicate primer/template (p/t) DNA (26,36). Pol V Mut contains an intrinsic DNA-dependent ATPase activity (36). Pol V Mut requires the presence of ATP/ATPγS to bind to p/t DNA, and ATP hydrolysis is involved in facilitating dissociation from DNA (36).

Many bacterial species, including pathogens, encode pol V (*umuDC*) homologs on their chromosomes. An additional highly conserved and surprisingly widespread pol V homolog is encoded on many ICEs, denoted *rumAB* (21,22). The ICEs that encode *rumAB* family pol's have the potential to migrate into many different bacterial species, including a range of important pathogens (21,22,37). However, these elements do not encode cognate *recA* genes and it is unclear whether they need to interact with the pathogenic host RecA protein to become fully functional. For example, Rum pol is active in the presence of *Ec recA1730* (S117F) (32) which is unable to activate *Ec* pol V (26,29,32,38) suggesting that either an interaction with RecA is not required for activation of Rum pol, or that Rum pol may be more promiscuous with RecA mutants, or homologs. The RumAB family polymerases produce a particularly high level of mutagenesis and are ∼3- to 10-fold more mutagenic than pol V (19,39). Thus, the regulation and activation of these enzymes has important implications for bacterial adaptation to antibiotics and other challenges that may be presented by a host.

In this paper, we have investigated the biochemical and mutagenic behavior of Rum DNA polymerase (Rum pol = RumA′$_2$B and also described as polV$_{R391}$ (40), which is a MEPol homolog of pol V encoded on the R391 ICE (19,37,39,41). We show that the active form of Rum pol is Rum Mut = RumA′$_2$B-RecA-ATP/ATPγS, which is analogous to pol V Mut (26). A critical general feature of Rum pol is that the horizontal transfer of R-plasmids and ICEs between different bacterial species implies the possibility that MEPols encoded by ICEs integrated into pathogen genomes might assemble by using RecA homologs promiscuously from a wide variety of recipient bacteria. To test this hypothesis, we have investigated the biochemical and *in vivo* mutagenic behavior of Rum Mut assembled with RecA homologs purified from seven bacterial species, four clinical bacterial isolates in which the *rumAB* encoding R391/SXT family of ICE's have been previously identified (*E. coli, V. cholerae, P. rettgeri, K. pneumoniae*) (22,42), and from three clinical isolates lacking *rumAB* genes (*P. aeruginosa, M. tuberculosis, S. aureus*). We have determined the extent to which Rum induced mutagenesis *in vivo* correlates with Rum Mut DNA polymerase activities *in vitro*.

MATERIALS AND METHODS

Strains and plasmids

Strains and plasmids are listed in Tables 1 and 2. The strain used for the mutagenesis experiments was RW616 [*lexA51*(Def) *ΔumuDC ΔrecA*]. This strain expresses all *lexA* (SOS) regulated genes constitutively. The deletion of *umuDC* and *recA* eliminates competition between the chromosomally encoded genes and homologs expressed from plasmids. Homologous *recA* genes were codon optimized for expression in *E. coli* (synthesized by GenScript). 5′ and 3′ linkers encoding *Nde*I and *Bam*HI sites were included at the initiation ATG codon and immediately downstream of the TAA termination codon, respectively and cloned into pJM1071 (Supplementary Figure S1A). This places the recombinant *recA* genes under the control of the *E.coli recAo281* operator constitutive promoter (43). RecA homologs from the following species were used in this study *(Genbank accession numbers)*: *E. coli* (NP_417179), *P. rettgeri* (WP_048608224*)*, *V. cholerae* (AAF93711), *K. pneumoniae* (YP_005228402), *P. aeruginosa* (NP_252307), *M. tuberculosis* (NP_217253) and *S. aureus* (YP_499795). Mutated variants of *Mt recA* (pJM1420 m1-m7) and *Ec recA* (pJM1421-M197D) were created using site-directed mutagenesis. For the mutagenesis experiments, RW616 was transformed with either two low-copy compatible plasmids expressing RumA′B and the various RecA homologs, or the entire 88kb R391 ICE encoding the *rumAB* operon together with the low-copy plasmids expressing the various RecA homologs. To assess Rum pol-dependent mutagenesis in the presence of chromosomal *umuDC, recA* and *lexA*, the entire R391 was moved into RW118 by bacterial conjugation.

Proteins

His-tagged Rum pol (RumA′$_2$B) was purified from *E. coli* RW644 strain carrying pARA1 (overexpressing untagged RumA′) and pHRB1 (expressing His-tagged RumB) according to the protocol previously described for pol V (34)**.** As noted above, each *recA* homolog was codon optimized for maximal expression in *E. coli* and recA genes from the various bacterial species were cloned into the *Nde*I-*Bam*HI sites of pET22b+ and expressed in RW1290 (Tables 1 and 2) and purified following the standard protocol for *Ec* RecA purification (44,45). The *Ec* RecA was purified from STL327 co-transformed with pAIR79 and pT7POL26 (44–46).

To site-specifically label *Ec* RecA with the Alexa Fluor 647 acceptor dye for smFRET experiments, the cross-linkable variant of *Ec* RecA-F21 *p*AzF (*p*AzpF*; p*-azido-L-phenylalanine) was expressed and purified. The *p*-azido-L-phenylalanine (pAzF) (47) was incorporated into the *Ec* RecA cloned in pAIR79 plasmid by replacing F21 with an amber codon (36), followed by co-transformation of pAIR79-*recA* F21*p*AzF with the vector pEVOL-pAZF (a gift from Dr Peter Schultz (The Scripps Research Institute, San Diego, CA) into the BLR expression strains (48). The *Ec* RecA-F21 *p*AzF protein was purified using the standard protocol for *Ec* RecA (44,45).

Rum Mut assembly

Rum Mut was assembled following the protocol established previously for pol V Mut and described in detail by Erdem *et al*. (36). Briefly, RecA nucleoprotein filament (RecA*) of the different bacterial species was assembled at 37°C with ATPγS on a 45 nt-dT ssDNA covalently attached

Table 1. Plasmids used in this study

Plasmid	Relevant characteristics	Source or reference
R391	Kan^R integrated into *prfC*	(19)
pGB2	low-copy-number, Spc^R vector	(70)
pCC1	pCC1BAC™, single copy Cm^R	Genscript GenBank:EU140750.1
pJM1388	single copy with *rumA′B* cloned into pCC1	This work
pJM1378	single copy with *rumAB* cloned into pCC1	This work
pJM1071	as pGB2 harboring the *Ec recAo281* promoter	(71)
pJM1421	as pJM1071 but with *Ec* codon optimized *recA* expressed from the *recAo281* promoter	This work
pJM1420	as pJM1071 but with *Ec* codon optimized *Mt recA* expressed from the *Ec recAo281*promotor	This work
pJM1428	as pJM1071 but with *Ec* codon optimized *Pa recA* expressed from the *Ec recAo281* promotor	This work
pJM1430	as pJM1071 but with *Ec* codon optimized *Sa recA* expressed from the *Ec recAo281* promotor	This work
pJM1451	as pJM1071 but with *Ec* codon optimized *Pr recA* expressed from the *Ec recAo281* promotor	This work
pJM1453	as pJM1071 but with *Ec* codon optimized *Vc recA* expressed from the *Ec recAo281* promotor	This work
pJM1455	as pJM1071 but with *Ec* codon optimized *Kp recA* expressed from the *Ec recAo281* promotor	This work
pJM1420-m1	As pJM1420 but expressing *Mt* RecA A76T	This work
pJM1420-m2	As pJM1420 but expressing *Mt* RecA A181N	This work
pJM1420-m3	As pJM1420 but expressing *Mt* RecA T188L	This work
pJM1420-m4	As pJM1420 but expressing *Mt* RecA D197M	This work
pJM1420-m5	As pJM1420 but expressing *Mt* RecA E230G, T231A	This work
pJM1420-m6	As pJM1420 but expressing *Mt* RecA D261Q	This work
pJM1420-m7	As pJM1420 but expressing *Mt* RecA A33R, R34S, Q35M, P36D	This work
pJM1421-M197D	As pJM1421 but expressing *Ec* RecA M197D	This work
pAIR79	pET21d(+)-*Ec recA*; Amp^R	(45)
pET22b+	medium copy, Amp^R, expresses proteins from an IPTG inducible T7 promoter	Novagen
pJM1440	pET22b-*Pr recA*; Amp^R	This work
pJM1442	pET22b-*Vc recA*; Amp^R	This work
pJM1443	pET22b-*Kp recA*; Amp^R	This work
pJM1475	pET22b-*Pa recA*; Amp^R	This work
pJM1474	pET22b-*Sa recA*; Amp^R	This work
pDH17	pET22b-*Mt recA*; Amp^R	This work
pARA1	high-copy (Amp^R) with untagged RumA′ expressed from the *Ara* promoter	(32)
pHRB1	low-copy (Kan^R) expressing His-tagged RumB	(32)
pAIR79-*recA*-F21pAzF	expressing *Ec* RecA-F21*p*AzF for site specific labeling	(36)
pSN5182/7	expressing PBP (phosphate-binding protein) protein for ATPase assay	(54,55)

Table 2. *E. coli* strains used in this study

Strain	Relevant genotype / phenotype	Source or reference
RW644	BL21(λDE3) derivative with *ΔumuDC596*::*ermGT ΔpolB1*::*Ωspec ΔdinB61*::*ble*	(34)
RW616	*thr-1 araD139 Δ(gpt-proA)62 lacY1 tsx-33 supE44 galK2 hisG4 rpsL31 xyl-5 mtl-1 argE3 thi-1 sulA211 lexA51*(Def) *ΔumuDC*::*ermGT ΔrecA306*::Tn*10*	This work
RW118	*thr-1 araD139 Δ(gpt-proA)62 lacY1 tsx-33 supE44 galK2 hisG4 rpsL31 xyl-5 mtl-1 argE3 thi-1 sulA211*	This work
RW1290	BL21(λDE3) derivative with *ΔumuDC596*::*ermGT ΔpolB1*::*Ωspec ΔdinB61*::*ble ΔrecA306*::Tn*10*	This work
STL327/pT7POL26	nuclease deficient (*exoI*$^-$ *exoIII*$^-$ *endoI*$^-$ *recJ*$^-$) with pT7POL26 (Kan^R) encoding T7 RNA polymerase under the control of a *lac* promoter	(44,45)
ANCC75	*leu purE trp his argG rpsL pho564 metA*	(54,55)

to Cyanogen Bromide Sepharose (with 3′-tip exposed) in small spin column (Bio-Rad). The unbound RecA and excess ATPγS was removed by extensive washes with 1× reaction buffer [20 mM Tris (pH 7.5), 8 mM $MgCl_2$, 5 mM DTT, 0.1 mM EDTA, 25 mM sodium glutamate and 4% (v/v) glycerol]. Rum pol was incubated with RecA*-beads followed by spin column centrifugation to separate Rum Mut from RecA*-beads (RecA* remains in spin column while Rum Mut is in flow-through). The concentration of Rum Mut was estimated by SDS-PAGE using purified RumA′, RumB and RecA as internal standards.

Rum Mut integrity

To verify that Rum Mut assembles as an intact stable physical complex composed of Rum pol (RumA′$_2$B) and RecA, we incorporated a His-tag on RumB to bind Rum Mut (or Rum pol) to a Ni^{2+}–NTA agarose (Qiagen) resin and to

analyze the bound complexes on SDS-page after extensive washes to remove adventitious proteins that did not assemble into the Rum Mut (or Rum pol) complex. If RecA is physically bound to Rum pol it will be eluted from the resin along with Rum pol. The protocol involves the following steps: 50 μl of 1.5 μM Rum Mut was diluted to 100 μl in 1× reaction buffer [20 mM Tris (pH 7.5), 8 mM $MgCl_2$, 0.1 mM EDTA, 25 mM sodium glutamate and 4% (v/v) glycerol] to reduce the concentration of DTT, followed by binding to 15 μl of Ni^{2+}–NTA agarose for 10 min at 37°C. The resin was washed 3 times with 100 μl of 1× reaction buffer. The bound proteins were eluted in 1× reaction buffer with 250 mM Imidazole and analyzed on SDS-page. The presence of three protein bands corresponding to RumB, RumA′ and RecA confirms the integrity and composition of Rum Mut complex.

DNA synthesis measurements *in vitro*

To verify that that Rum Mut (Rum pol-RecA-ATP) is an active stand-alone form of Rum pol able to synthesize DNA in the absence of a RecA nucleoprotein filament (RecA*), we measured the activities of Rum Mut and homologs of Rum Mut assembled with RecA homologs. DNA synthesis was measured on a 5′-^{32}P-labeled primer template hairpin (HP) with a 3-nt overhang (oh) 5′-AGA GCA GTT AGC GCA TTC AGC TCA TAC TGC TGA ATG CGC TAA CTG C-3′ (Supplementary Figure S1B). This p/t DNA construct was used, rather than for example two ssDNA oligomers annealed to form a p/t DNA, to eliminate the possibility of the formation of RecA* that could assemble by the binding of free RecA to free ssDNA in solution. The 3 nt ssDNA template oh cannot support the assembly of RecA* on the template strand. We previously showed that the addition of excess free RecA + ATP/ATPγS to the 3 nt overhang p/t hairpin was unable to support RecA* transactivation of pol V (28), which further showed that RecA* nucleoprotein filament formation was not occurring. Rum Mut (400 nM) was added to the reaction containing 50 nM 3 nt oh HP p/t DNA DNA, 500 μM ATP/ ATPγS, dNTP substrates [mix of dTTP, dGTP, dCTP, (500 μM each) and 1× reaction buffer (20 mM Tris (pH 7.5), 8 mM $MgCl_2$, 5 mM DTT, 0.1 mM EDTA, 25 mM sodium glutamate and 4% (v/v) glycerol]. The reactions were incubated at 37°C for 60 min and were terminated by the addition of stop solution containing 20 mM EDTA in 95% formamide. The p/t DNA reaction products were resolved on a 20% + 8 M urea denaturing polyacrylamide gel allowing detection of single nucleotide incorporation to p/t DNA. Gel band intensities were measured by phosphorimaging and quantified using Image Quant software. The fraction of extended primer (% PE) was calculated by integrating the band intensities of extended primer DNA divided by the total integrated DNA band intensity. A similar protocol was used to measure Rum pol activity. The RecA* gel lanes refer to the inclusion of the RecA nucleoprotein filament in the reaction to transactivate the mutasome. Mutasome specific activities (ng DNA primer extended/min/ng protein) were determined within the linear range of time (≤30 min) and enzyme concentration (200–600 nM). Each experiment was repeated 4 times (Supplementary Table S1).

Spontaneous and MMS-induced mutagenesis measurements

Quantitative spontaneous mutagenesis assay. To assess the effect of RecA homologs on Rum pol mutagenesis, *E. coli* strain RW616 [*lexA51*(Def) *ΔumuDC ΔrecA*] was transformed with two plasmids; one expressing RumA′B, or the entire R391 ICE and a second plasmid expressing RecA homologs (Table 1). To measure the frequency of spontaneous reversion of the *hisG4*(Oc) allele, three individual colonies of each strain were grown overnight at 37°C in 5 ml LB medium containing appropriate antibiotics. The next day, cultures were harvested by centrifugation and resuspended in an equal volume of SM medium (49). One hundred microliters of the resuspended pellets were spread on five low-histidine minimal plates [Davis and Mingioli minimal agar plates (50) plus glucose (0.4% wt/vol); agar (1% wt/vol); proline, threonine, valine, leucine and isoleucine [all at 100 μg ml^{-1}); thiamine (0.25 μg ml^{-1}); and histidine (1 μg ml^{-1})]. After incubating the plates for four days at 37°C, the His^+ mutant colonies were counted and averaged between the independent cultures and standard error of the mean (SEM) was calculated. To assess Rum pol-dependent mutagenesis in the presence of chromosomal *umuDC, recA* and *lexA,* R391 was moved into RW118 by bacterial conjugation, and the frequency of spontaneous and MMS-induced His^+ revertants were calculated as described above.

Qualitative MMS-induced mutagenesis assay. In a similar manner to the spontaneous mutagenesis assay, harvested and SM-resuspended cultures were plated onto low-histidine minimal plates. A sterile filter disk was placed onto the middle of the agar plate and 5 μl of a one to five dilution of methyl methane sulfonate (MMS) in dimethylsulfoxide (DMSO) was spotted onto the filter disk. After 4 days of incubation, the plates were imaged.

RecA*-mediated RumA cleavage to RumA′

The ability of various homologs of RecA* to cleave RumA to RumA′ was detected by Western blots performed on cell lysates from Ciprofloxacin treated RW616/pJM1378 *E. coli* strains expressing a homolog of RecA. Over-night cultures were diluted in fresh Luria-Bertani media and grown to mid-log phase (OD ∼ 0.5) at 37°C, followed by treatment with 30 ng/ml Ciprofloxacin (DNA damaging antibiotic) for 3 h. Both untreated and cipro-treated cultures were harvested by centrifugation, resuspended in NuPage LDS sample buffer (Novex) and freeze-thawed to produce whole cell extracts. Extracts were electrophoresed on NuPage 4–12% Bis–Tris gels (Novex) and subsequently transferred to an Invitrolon PVDF membrane (Novex). These membranes were probed with an appropriate dilution of purified rabbit anti-RumA antibodies and then probed with an appropriate dilution of Goat Anti-Rabbit IgG (H + L)-AP Conjugate (Biorad). Using the CDP-Star chemiluminescent assay (Tropix), the RumA/A′ proteins were visualized utilizing a FlourChem HD2 imager (Alpha Innotech). The band intensities corresponding to RumA and RumA′ were quantified using Image Quant software and the fraction of RumA cleavage (% PE) was calculated by integrating the band intensity corresponding to RumA′ divided by the total integrated band intensities.

Measurements of Rum Mut-dependent TLS

To measure effect of the β-clamp on Rum Mut processivity and translesion synthesis (TLS) we constructed a circular p/t DNA with an abasic site located on the template strand 30 nt downstream from the p/t DNA junction. The circularized 90 nt template [5′P-ATG ACA AGA CAA GAC **X**AG ACA AGA CAA GAC AAG ACA AGA CAA GAC AAG AAA TCA CCT TCA TCC AAA TCC ACT AAA CCA TAT CCA TCC TCG-3′] was annealed to a P^{32}-5′- labeled 20 nt primer [P^{32}-5′-TTT GGA TGA AGG TGA TTT CT-3]'; with the 20 nt annealed region shown underlined in the 90 nt template. **X** refers to an abasic site that was introduced in the template strand by placing an internal dSpacer (1′,2′-dideoxyribose, Integrated DNA Technologies). A detailed protocol for synthesis of the circular p/t DNA is contained in Sikand *et al.* (51). Since the β-clamp can slide-off the ends of linear p/t DNA, the circular p/t DNA allows for stable binding of β-clamp to DNA. Loading and removal of the β−clamp at the 3′-OH-p/t junction is carried out by the γ-clamp loading complex. The circular p/t DNA (25 nM) was incubated for 1 min at 37°C with β-clamp (200 nM) and γ-complex (150 nM) and with 500 uM ATP/ATPγS in standard 1× reaction buffer (20 mM Tris (pH 7.5), 8 mM $MgCl_2$, 5 mM DTT, 0.1 mM EDTA, 25 mM sodium glutamate and 4% (v/v) glycerol) followed by the addition Rum Mut-*Ec* (400 nM) and saturating concentration of dNTPs (mix of dATP, dTTP, dGTP, dCTP 500 μM each). Small aliquots were taken out at appropriate time points and reactions were terminated by the addition of a stop solution containing 20 mM EDTA in 95% formamide. The products of the reactions were separated on 20% denaturing PAGE gel. Gel band intensities were measured by phosphorimaging and quantified with Image Quant software, and the fraction of extended primer (% PE) was calculated by integrating the band intensities of extended primer DNA divided by the total integrated DNA band intensity. The Rum-*Ec* dependent TLS measurements were repeated 3 times.

Labeling of p/t DNA and RecA for smFRET

The p/t DNA for smFRET studies was assembled using 40 nt 5′-T-biotinylated primer (5′ Biotin-TCG AGG ATG GAT ATG GTT TAG TGG ATT TGG ATG AAG GTG A-3′) and 54 nt template with internal C6-dT-amino modification for Alexa Fluor 555 (AF555) labeling (5′-TAG CAT GCG TCA GCT TCA CC**T-(AF555)** TCA TCC AAA TCC ACT AAA CCA TAT CCA TCC TCG-3′). DNA oligos were purchased from Integrated DNA technologies and purified in-house on denaturing PAGE. The template oligo was labeled with NHS-ester-AF555 (ThermoFisher) by incubating molar excess of dye (5×) with the template (1×) overnight at room temperature and protected from light. The free dye is removed by ethanol precipitation and the DNA was purified by running denaturing PAGE gels to separate labeled DNA with unlabeled DNA. The labeling efficiency of final AF555-template stock was 100% as estimated by spectrophotometer. Prior to the smFRET experiments, 5′-biotinylated primer was annealed to the AF555-template at a ratio of 1:1 by heating to 55°C and allowed to slowly cool to 16°C by decreasing 1°C per minute in a thermocycler. The AF555 fluorophore serves as a donor in smFRET experimental set-up, and upon excitation with a 561 nm laser, its emission energy is transferred to an AF647 accepter fluorophore present on the RecA subunit of Rum Mut, which subsequently fluoresces when located approximately ≤10 nm from donor.

To site specifically label *Ec* RecA with Alexa Fluor 647 (AF647), we used a cross-linkable variant of RecA-F21 *p*AzF (*p*AzpF*;* *p*-azido-L-phenylalanine). Purified RecA-F21 *p*AzF was incubated with a molar excess (1:5) of Alexa Fluor 647 DIBO Alkyne (AF647; ThermoFisher Scientific) in 20 mM Tris, 0.1 mM EDTA, 10% glycerol pH 7.5 buffer and rotated at 4°C overnight. To remove free dye and separate the labeled protein from the unlabeled fraction, the protein mixture was loaded onto a Ceramic Hydroxyapatite (Bio-Rad) column and eluted with a phosphate gradient from 0 to 0.25M potassium phosphate. Unbound dye is eluted in the initial zero phosphate column wash, while AF647-labeled RecAF21*p*AzF elutes early during the potassium phosphate gradient followed by unlabeled *Ec* RecA which elutes last. Labeled RecA concentrations and labeling efficiency were determined via spectrophotometry at 280 and 650 nm, respectively. RecA labeling efficiency was about 60%. AF647-labeled RecAF21*p*AzF was used to assemble Rum Mut for the smFRET measurements.

Single-molecule FRET measurements

smFRET microscopy was used to visualize the binding of Rum Mut to p/t DNA in real-time in either the presence or absence of ATP. As described above, the smFRET donor-acceptor pair (labeled p/t DNA with AF555 donor, introduced internally into DNA template strand annealed to a primer tethered to a glass coverslip) and AF647 acceptor on Rum Mut-*Ec* RecA) were excited with 561 nm wavelength laser light. Upon donor excitation, the binding of AF647-Rum Mut-*Ec* to p/t DNA is detected as an increase in emission of acceptor fluorophore that counter-correlates with a decrease of a donor emission.

The smFRET analysis was performed as follows. High precision microscope glass coverslips (Marienfeld, #1.5, Ø25 mm) were first cleaned by sonication in ddH_2O for 1 min, followed by treatment with 100 mM KOH for 20 min. Then, slides were cleaned in Piranha solution (H_2O_2:H_2SO_4 is 1:3) for 4 min, followed by sonication in ddH_2O for 10 min, followed by incubation in a solution containing 3 ml of 3-aminopropyltriethoxysilane (Sigma-Aldrich), 5 ml acetic acid, and 100 ml methanol for 30 min, with 1-min sonication in the middle of the incubation. The cleaned slides were rinsed with ddH_2O and air-dried prior to incubation for 16 h in solution containing 25 mM 5:1 (v/v) polyethylene glycol (PEG) and biotin-PEG-succinimidyl valerate (Laysan Bio) in 0.1 M sodium bicarbonate pH 8.3 buffer. To reduce any possible background fluorescence (52), a second round of surface pegylation was done for 2 h using 25 mM of 4-methyl-PEG-NHS-ester (Thermo-Fisher). Coverslips were then washed with ddH_2O and incubated with streptavidin (Sigma) for 10 min in a buffer containing 20 mM Tris–HCl, 50 mM NaCl pH 7.5 followed by 5 min blocking using 1× blocking buffer (100 mM Tris–HCl pH 7.5, 10 mM EDTA, 250 mM NaCl, 2.5 mg/ml BSA and 0.0125% v/v

Tween 20). Finally, the coverslips were washed and coated with 5–10 pM AF555-labeled p/t DNA for 5 min. Unbound p/t DNA was washed off using imaging buffer containing 1× reaction buffer without DTT (20 mM Tris (pH 7.5), 8 mM $MgCl_2$, 0.1 mM EDTA, 25 mM sodium glutamate and 4% (v/v) glycerol) and with 50 μg/ml BSA, 2 mM Trolox, 10 mM PCA and 100 nM PCD (53). Rum Mut was assembled with AF647-RecA F21*p*AzF and added to the coverslip at 1–5 nM. To assess AF647-Rum Mut-*Ec* binding to AF555- labeled p/t DNA, Rum Mut-*Ec* alone or activated with 500 μM ATP or ATPγS was added at $t = 30$ s after start of image acquisition.

Fluorescence imaging was performed on an inverted Nikon Eclipse Ti-E microscope equipped with total internal reflection optics, 561 and 647 nm fiber-coupled excitation lasers (Agilent), a ×100 1.49 NA objective, a two-camera imaging splitter (Andor) and two iXon EMCCD cameras (Andor). A multi-band pass ZET405/488/561/647x excitation filter (Chroma), a quad-band ZT405/488/561/647 dichroic mirror (Chroma), an emission splitting FF-640-FDi01 dichroic mirror (Semrock) and two emission filters at 600/50 nm (Chroma) and 700/75 nm (Chroma) for AF555 p/t DNA and AF647-Rum Mut respectively, were used. smFRET images were acquired using 561 nm laser excitation at an image acquisition rate of 300 ms/frame in each channel. Channel alignment was performed using a few 40 nm TransFluoSphere beads (488/685 nm, Life Technologies) as fiducials markers.

To calculate smFRET efficiencies the 8 × 8 pixel region of interests was drawn around individual p/t DNA molecules in overlaid two-color images, and signal intensity from both channels were extracted for each acquisition frame. Automated detection of countercorrelated smFRET signals on the slides were performed using in-house AI software. FRET efficiency was calculated using the formula: $E = I_A/(I_D + I_A)$, where I_D is the signal intensity from an individual AF555-labeled p/t DNA molecule and I_A is the signal intensity of a bound AF647-Rum Mut in each frame. The smFRET DNA binding efficiencies were presented as histograms by binning the smFRET values for multiple individual smFRET binding events, which proscribes the distance between the donor (p/t DNA) and acceptor (pol V Mut RecA subunit) fluorophores.

Rum Mut and RecA-dependent P_i release caused by the hydrolysis of the mutasome-associated ATP

The ATPase activity of Rum Mut was measured using a highly sensitive MDCC-PBP assay which allows a real-time measurement of inorganic phosphate (Pi) release arising from ATP hydrolysis (54,55). *E. coli* phosphate-binding protein (PBP) was purified and labeled with MDCC fluorophore (Sigma-Aldrich) as described previously (54,55). Binding of P_i (phosphate) to MDCC-PBP is rapid and tight ($K_d \sim 0.1$ μM) and results in large increase of MDCC fluorescence (55). Using a QuantaMaster (QM-1) fluorometer (Photon Technology International), the change in fluorescence of MDCC-PBP was detected in real-time. Wavelengths for excitation and emission of the MDCC were selected using monochromators with a 1-nm band pass width and were set at 425 and 464 nm, respectively. A 65 μl of reaction contains 5 μM MDCC-PBP, 1 μM DNA, 0.05 units/ml PNPase, 100 μM 7-methylguanosine and various concentrations of Rum Mut, or RecA. PNPase and 7-methylguanosine were used to remove any traces of Pi prior ATP hydrolysis. ATP hydrolysis was initiated by adding a 5 μl of ATP stock to 500 μM final concentration and the measurements were taken at 1 point per sec resolution for 900 s. The maximum rate (V_{max}) of P_i release was derived from the linear slope of Pi release, and k_{cat} was calculated by dividing V_{max} by the enzyme concentration. Each measurement was repeated 2–3 times.

RESULTS

Assembly of an activated Rum Mutasome containing *E. coli* RecA and ATP

E. coli pol V ($UmuD'_2C$) lacks detectable catalytic activity (27–29,35). To perform DNA synthesis, pol V must bind a RecA monomer, transferred from the 3′-proximal tip of a RecA nucleoprotein filament (RecA*), and then to a molecule of ATP (or ATPγS) to assemble as an activated mutasomal complex, pol V Mut = $UmuD'_2C$-RecA-ATP/ATPγS (26,36). Essential for the assembly of pol V Mut is the transfer of a RecA monomer from the 3′-proximal end of RecA* to pol V (26,28,32,38). The interaction surface for RecA includes the amino acids N113-S117, which are accessible to pol V when transferred as a RecA monomer from the 3′-proximal end of RecA* to form pol V Mut (32).

In a process identical to the activation of pol V Mut (26,36), Rum Mut is formed by transfer of a RecA molecule from RecA* to $RumA'_2B$ (Rum pol), followed by binding of an ATP (or ATPγS) monomer to form Rum Mut (Figure 1A). To show that Rum Mut assembles as a physical complex of Rum pol and RecA we bound Rum Mut, containing a His tag on RumB, to a Ni^{2+}–NTA resin (Figure 1B, C), and washed the resin extensively to remove non-Rum Mut contaminants (see Materials and Methods). Visualization of the eluted Ni^{2+}–NTA bound complex by SDS-PAGE showed 3 gel protein bands corresponding to RumB, RumA′, and RecA (Figure 1B, C) confirming Rum Mut integrity. Rum pol, by itself, cannot synthesize DNA (Figure 1D), but incubation of Rum pol with RecA* converts Rum pol into an active mutasome that copies DNA (Figure 1D, + RecA*). Rum Mut cannot synthesize DNA in the absence of ATP or ATPγS (Figure 1E). Rum Mut performs robust DNA synthesis with slowly-hydrolysable ATPγS, 99% primer extension (PE) but has much lower activity with ATP (6% PE) (Figure 1E). We have used a primer/template (p/t) DNA in the form of a hairpin (HP) containing a 3 nt long template overhang (oh) (Figure 1D, E; Supplemental Figure 1B) to ensure that transactivation of Rum pol by RecA* is not taking place and that the polymerase activity is present in a stand-alone mutasome. RecA* cannot assemble on the 3 nt oh (56,57) and the use of a self-annealing p/t DNA effectively eliminates the presence of adventitious ss-DNA that could serve as a transactivating RecA*.

To link the template replication properties of the mutasome to general polymerase studies, synthesis by Rum Mut was measured on circular p/t DNA, containing an abasic

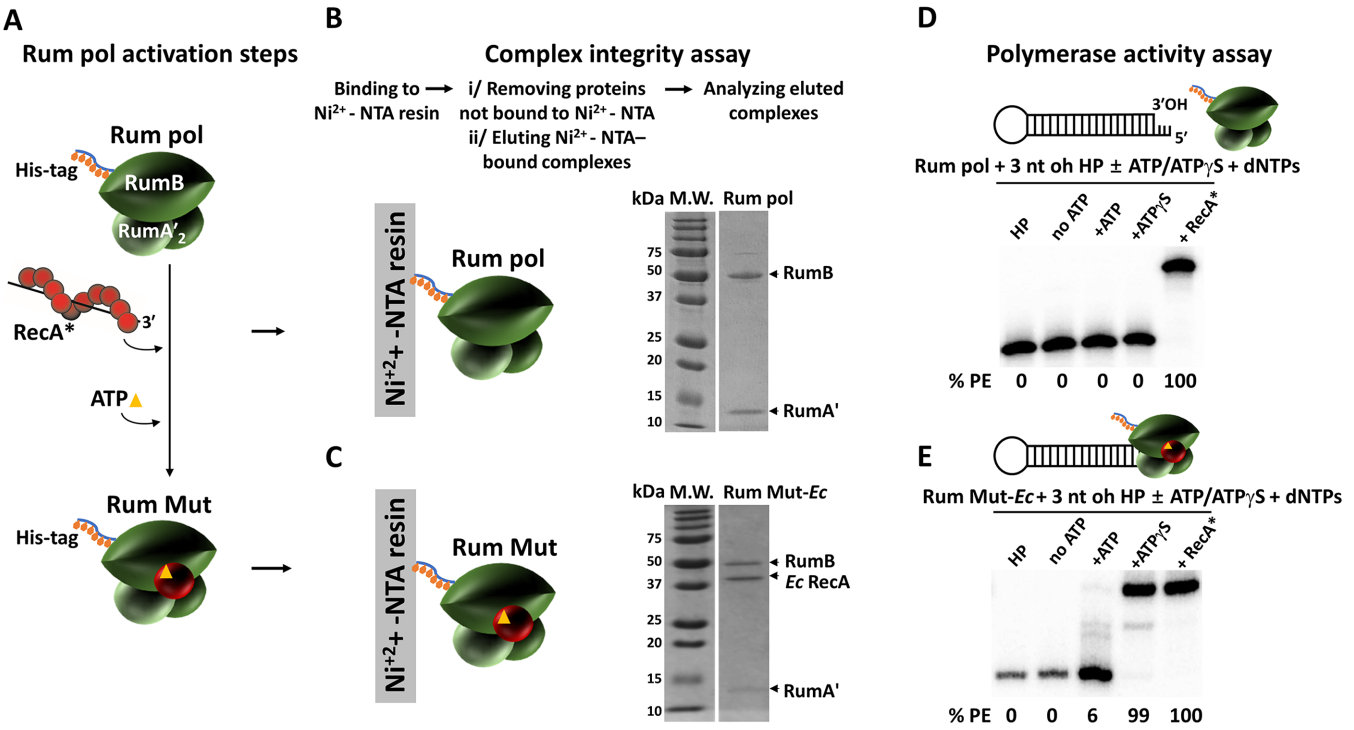

Figure 1. Rum Mut is an activated form of pathogen-encoded Rum polymerase. (**A**) Sketch showing the conversion of inactive Rum pol (RumA′$_2$B) to an activated mutasome by the transfer of a RecA monomer from the 3′-tip of RecA* followed by the binding of a molecule of ATP to form Rum Mut = RumA′$_2$B-RecA-ATP. Rum Mut is catalytically active in the absence of RecA*. (**B, C**) Rum Mut integrity analysis. To show that Rum pol and RecA assemble as a physical complex, Rum Mut (and Rum pol), containing a His tag on RumB, was bound to a Ni^{2+}-NTA resin and washed extensively to remove proteins not associated with the complex. An SDS-page analysis of the eluted complex showed 3 gel protein bands for Rum Mut corresponding to RumB, RumA′ and RecA, thus confirming the integrity of the mutasomal complex. (**D, E**) Activity of Rum pol and Rum Mut measured on p/t DNA in the presence and absence of ATP or ATPγS. The 'RecA*' lane shows transactivation of Rum pol in the presence of RecA*. % PE refers to percent of p/t extended, *Ec* RecA is *E. coli* RecA and Rum Mut-*Ec* refers to Rum Mut complex assembled with *Ec* RecA. The reactions (1 h, saturating dNTP concentrations) were carried out on hairpin (HP) p/t DNA with a 3 nt template overhang (oh), radioactively-labelled with ^{32}P at the 5′-template-end (see Materials and Methods).

template lesion (X), in the presence and absence of the β-processivity clamp (Figure 2). In the absence of β, Rum Mut synthesizes DNA with ATP (10% at 2h; (Figure 2B, first panel) and ATPγS (16% at 2h; (Figure 2B, third panel) but remains stalled at X. Translesion synthesis (TLS) occurs with ATPγS in the presence of β clamp enabling synthesis to reach the end of the template in the absence of transactivating RecA* (Figure 2B, fourth panel). β clamp stimulates Rum pol activity with ATP, but in contrast to ATPγS, the presence of transactivating RecA* is required for TLS and downstream synthesis (Figure 2B, second panel).

TIRF-FRET visualization of ATP-dependent mutasome binding to DNA

The activated form of pol V Mut contains the presence of a single molecule of ATP or ATPγS (26), which is required for binding the mutasome to p/t DNA at the primer 3′-end (36,58). We have used single-molecule (sm) TIRF-FRET microscopy to visualize the binding of Rum Mut-*Ec* to p/t DNA in real-time (Figure 3, Supplementary Movie S1–S3). An Alexa Fluor 555 (AF555) fluorescent donor molecule was placed internally on template strand of a p/t DNA attached to glass coverslip and an Alexa Fluor 647 (AF647) fluorescent acceptor molecule was placed on RecA subunit of Rum Mut (Figure 3A; sketch). Upon excitation of the donor dye, binding of Rum Mut to p/t DNA is detected as an increase in the emission of the acceptor dye that is precisely counter-correlated with a decrease in the donor emission signal (Figure 3C, D). The FRET efficiency and distribution (0.2–1.0, peak at 0.7, Figure 3E) corresponds to a range of binding distances of 49 to 64 Å between the donor and acceptor fluorophores. The smFRET data provide conclusive evidence that ATP must be present in the reaction to allow the formation of an activated Rum Mut complex that binds to p/t DNA (Figure 3C, D, Supplementary Movies S2 and S3). The inactive mutasome lacking ATP cannot bind to p/t DNA (Figure 3B, Supplementary Movie S1), in agreement with TIRF-FRET data for pol V Mut (58).

A propos of its requirement to have a bound adenine nucleoside triphosphate cofactor (ATP or ATPγS) for binding the mutasome to p/t DNA, Rum Mut also contains an intrinsic DNA-dependent ATPase activity with properties that mimic those observed for pol V Mut (36) (Supplementary Figure S2). The catalytic rate constant for Rum Mut [$k_{cat} = 169 \pm 4.5 \times 10^{-3}$] is similar to pol V Mut [$k_{cat} = 160 \pm 5.0 \times 10^{-3}$, (36)]. As observed previously for pol V Mut, the Rum Mut ATPase remains active when assembled with an *E. coli* RecA mutant (E38K/K72R) (Supplementary Figure S2B); the K72R mutation is located

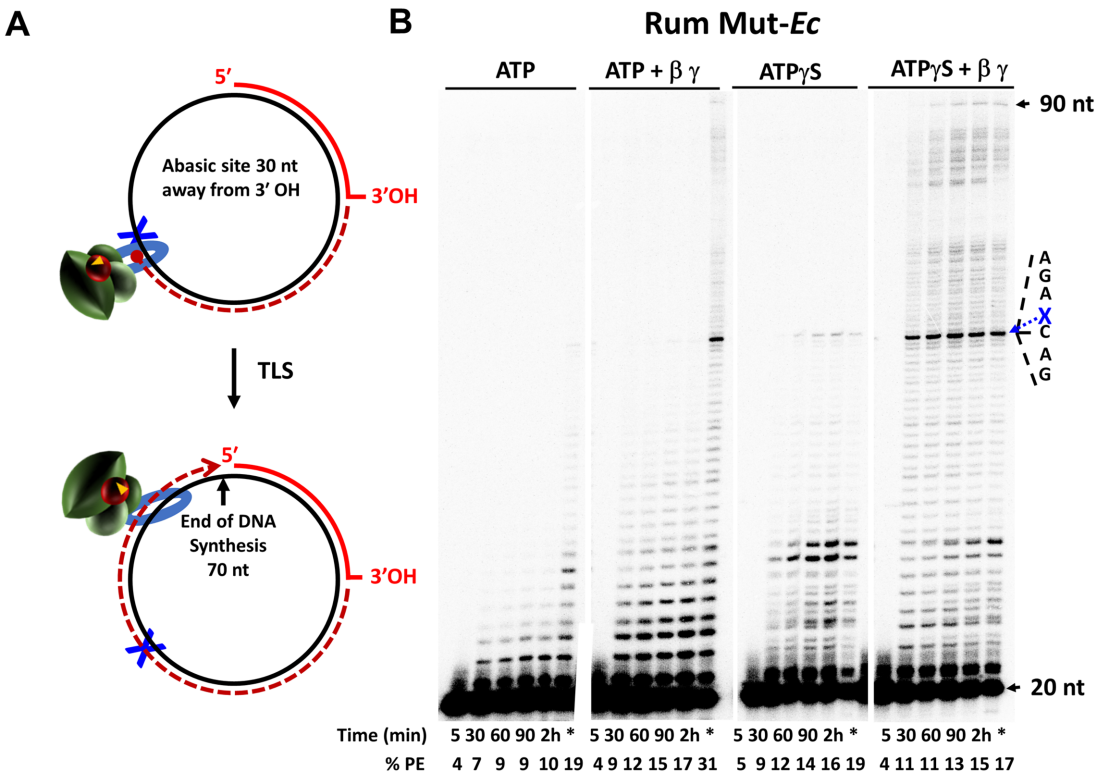

Figure 2. Effect of β-processivity clamp on TLS activity of Rum Mut-*Ec*. (**A**) Sketch showing experimental set up. Briefly, β -clamp is loaded on circular p/t DNA with γ-complex and ATP/ATPγS prior adding Rum Mut-*Ec* and dNTPs. The circular p/t DNA contains a template abasic site (X) located 30 nt downstream of the 3′OH p/t junction. (**B**) The polymerase activity of Rum Mut-*Ec* (400 nM) was measured with 20-nt primer/ 90-nt circular template (25 nM) in the presence of a saturating concentration of ATP or ATPγS (500 μM) and dNTP's (500 μM each). The β-clamp and γ-complex are present in excess relative to DNA at 200 nM and 150 nM concentrations, respectively. (X) represents the location of the abasic site in the sequence shown at the right-hand side of the gels. (*) represents reaction lane (last in each panel) where *trans*-RecA* has been added at $t = 2$ h.

in the Walker A motif, which completely inactivates the DNA-dependent ATPase activity of *E. coli* RecA* (59). As shown previously, the biochemical consequence of the DNA-dependent ATPase is to dissociate pol V Mut from p/t DNA (36). If this analogy holds for Rum Mut, the strongly reduced deoxynucleotide incorporation activities of the Rum Mut-*Ec* bound to ATP may be principally caused by rapid ATP hydrolysis causing Rum Mut-p/t dissociation, which does not occur in mutasomes assembled with slowly-hydrolysable ATPγS.

Activity of Rum pol in a range of bacterial species

Since Rum pol is encoded on an ICE that can be transferred between Gammaproteobacteria bacterial species (21,22,37), it seems reasonable to expect that it should be able to bind a variety RecA monomers along with a molecule of ATP to become activated for DNA synthesis in the host species. To test this hypothesis, we performed a series of *in vitro* and *in vivo* experiments with Rum Mut assembled with RecA homologs from four clinical bacterial isolates in which RumAB encoding ICE's have been previously identified (*E. coli, V. cholerae, P. rettgeri, K. pneuomniae*), and from three clinical bacterial isolates lacking *rumAB* genes (*P. aeruginosa, M. tuberculosis, S. aureus*).

We used the ClustalW algorithm in a MacVector (version 18.1.1) and a SplitsTree4 (version 4.14.4) to perform a multi sequence alignment (Figure 4A) and to generate an unrooted phylogenetic tree for each RecA homolog (Figure 4B). The analysis revealed phylogenetic relatedness of *E. coli* (*Ec*), *V. cholerae* (*Vc*), *P. rettgeri* (*Pr*), *K. pneumoniae* (*Kp*) and *P. aeruginosa* (*Pa*) RecA's which share more than 70% protein sequence identity while RecA's of *M. tuberculosis* (*Mt*) and *S. aureus* (*Sa*) are phylogenetically more distant and share 61% and 58% sequence identity with *Ec* RecA, respectively. We have posed three questions relating to the phylogeny mapping: 1) Do the phylogenetic differences between RecA homologs impact their ability to interact with Rum pol and form active Rum mutasomes? 2) Do mutasomes assembled with RecA homologs require activation by ATP or ATPγS? 3) Do the frequencies of mutations induced by Rum pol *in vivo* correlate with Rum Mut DNA polymerase activities measured biochemically?

Analysis of Rum Mut assembled using RecA purified from different bacterial species and effects of ATP/ATPγS

We used purified RecA proteins to assemble Rum Mut's *in vitro* (36). Rum Mut activity was measured on 3 nt overhang (oh) hairpin (HP) DNA in the absence and presence of saturating concentrations of ATP/ATPγS and dNTPs. We found that the RecA homologs, with the exception of *Sa* RecA, were able to form Rum Mut complexes that became

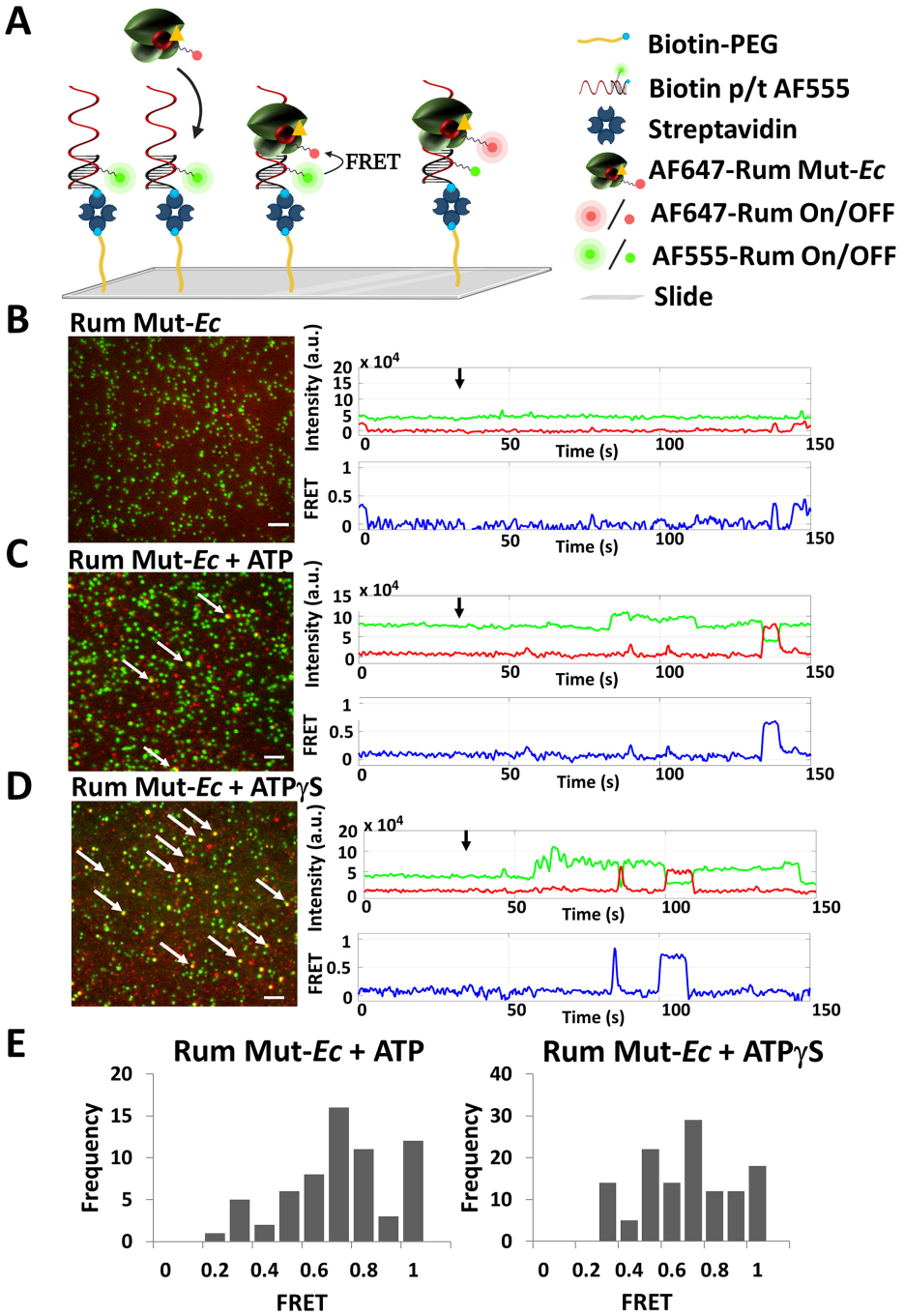

Figure 3. ATP-dependent binding of Rum Mut-*Ec* to p/t DNA visualized in real-time at single-molecule resolution. (**A**) Sketch of smFRET experimental setup (created using BioRender.com). An AF555 donor-labeled p/t DNA linked to streptavidin-biotin is attached to a glass slide surface. Binding of AF647 acceptor-labeled Rum Mut-*Ec* to p/t DNA is observed as an increase in emission of the acceptor fluorophore that counter-correlates with a drop of a donor emission. (**B–D**) Representative smFRET images and individual FRET trajectories of ATP/ATPγS-dependent binding of Rum Mut-*Ec* to p/t DNA. AF555-labeled p/t DNA molecules are shown as green spots in the smFRET images and un-bound AF647–Rum Mut-*Ec* molecules in solution are shown as red spots (B-D left panels). Binding events are represented as yellow/orange colocalized AF647- Rum Mut-*Ec* and AF555-labeled p/t DNA signals. A subset of representative binding events is indicated by the arrows. The white bar is equivalent to a 25 pixels length (4 pixels width) where 1 pixel = 107 nm. The microscope view is 512 × 512 pixels, and the images shown are portions of that view. Representative smFRET trajectories show donor and acceptor emissions (green and red) throughout the time-scale of image acquisition along with calculated FRET efficiencies in blue. Not-activated (B) or ATP/ATPγS activated (C, D) AF647- Rum Mut-*Ec* was added to the slide at $t = 30$ s after the start of image acquisition (indicated by arrow) and data were collected for up to 5 min, prior to the onset of photobleaching. The smFRET trajectories (B–D) show the initial 150 s of data acquisition. Rum Mut-*Ec* does not bind p/t DNA in the absence of ATP/ATPγS (B and Supplementary Movie S1). The addition of ATP (C and Supplementary Movie S2) or ATPγS (D and Supplementary Movie S3) activates Rum Mut-*Ec* enabling binding of the mutasome to DNA. (**E**) Histogram showing smFRET efficiencies corresponding to the binding of ATP/ATPγS-activated Rum Mut to AF555-labeled p/t DNA. The FRET efficiency is calculated as $E = I_A/(I_D + I_A)$, where I_A and I_D represent acceptor and donor emission, respectively. The histogram represents the smFRET distribution for 64 DNA binding events of Rum Mut-*Ec* + ATP and 127 binding events of Rum Mut-*Ec* + ATPγS.

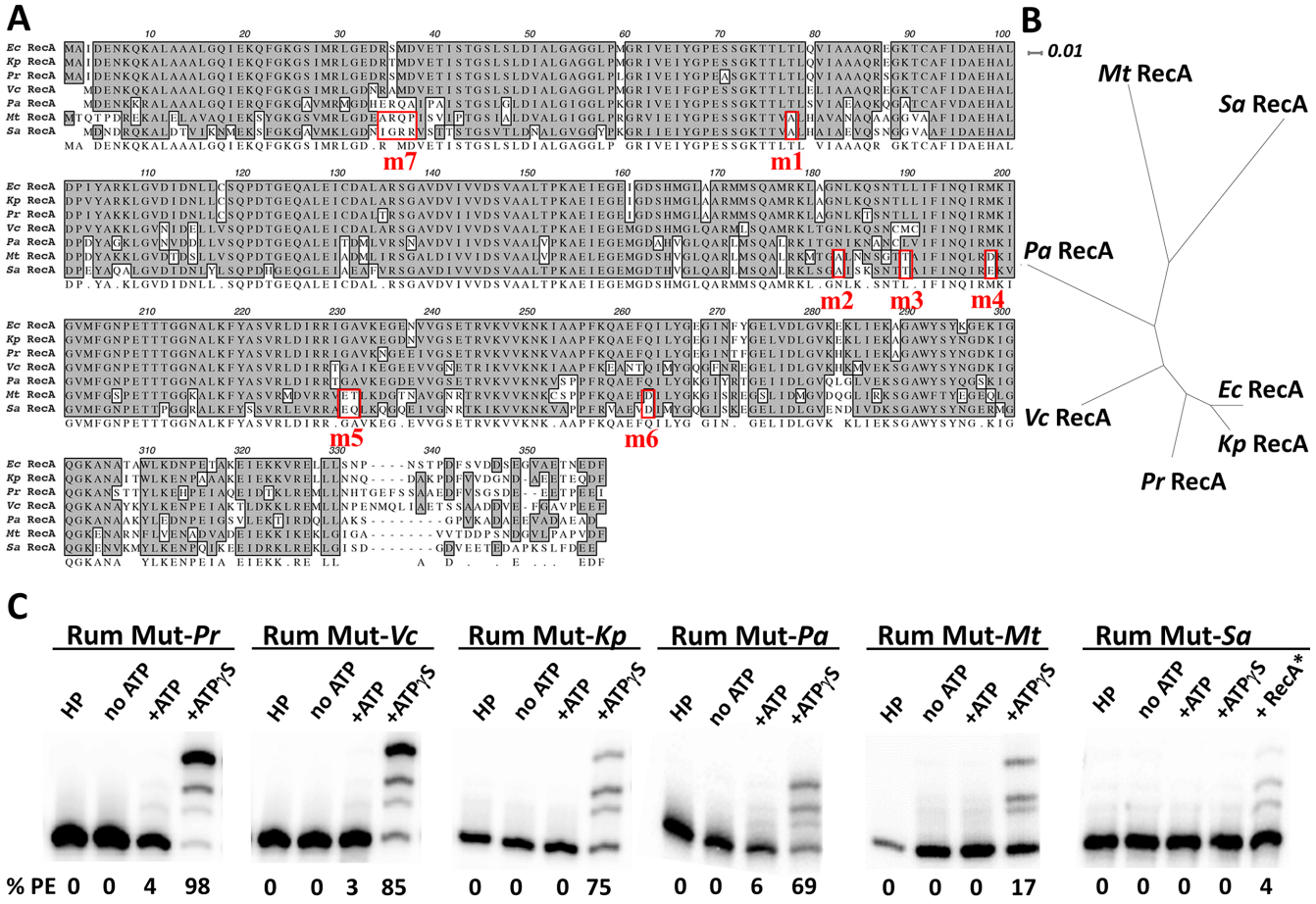

Figure 4. RecA homologs from variety of bacterial pathogens form Rum Mut complexes that require activation by ATP or ATPγS for DNA synthesis. (**A**) A ClustalW multiple sequence alignment of RecA homologs encoded by different bacterial pathogens. Protein sequences were obtained from Genbank sequence files: NP_417179 (*Ec* RecA); YP_005228402 (*Kp* RecA); WP_048608224 (*Pr* RecA); AAF93711 (*Vc* RecA); NP_252307 (*Pa* RecA); NP_217253 (*Mt* RecA); YP_499795 (*Sa* RecA). Identical or highly conserved amino acid residues are shaded and blocked together. Amino acid differences present in both *Mt* RecA and *Sa* RecA, which form weakly active Rum Mut-*Mt* and inactive Rum Mut-*Sa*, are highlighted in red. (**B**) An unrooted phylogenetic tree indicating the evolutionary relatedness of RecA homologs. The scale bar corresponds to an estimated amino acid substitutions per site of 0,01 (the number of substitutions divided by the length of the sequence). (**C**) Activity of Rum Mut assembled with RecA homologs measured for 1 h on 3 nt oh HP DNA in the absence and presence of activating ATP/ATPγS and with saturating concentration of dNTPs. All RecA homologs, with the exception of *Sa* RecA, form active Rum Mut complexes that require activation with ATP/ATPγS for DNA synthesis. The 'RecA*' lane shows transactivation of Rum pol in the presence of RecA*. Rum Mut-*Pr*, Rum Mut-*Vc*, Rum Mut-*Kp*, Rum Mut-*Pa*, Rum Mut-*Mt* and Rum-*Sa* abbreviations refer to the identity of bound RecA homologs.

activated for DNA synthesis upon addition of ATP/ATPγS (Figure 4C). Using Rum Mut-*Ec* (Figure 1E, +ATPγS, 99% PE) as a benchmark for comparison with the other RecA homolog mutasomes (Figure 4C, ATPγS lane), we found that two of them were comparably active, Rum Mut-*Pr* 98% PE; Rum Mut-*Vc*, 85% PE, two exhibited slightly reduced activity, Rum Mut-*Kp*, 75% PE and Rum Mut-*Pa* (69% PE), while Rum Mut-*Mt* had substantially reduced activity (17% PE). Rum Mut assembled with phylogenetically distant *Sa* RecA was not active as a stand-alone mutasome in the presence of ATP/ATPγS but shows weak activity when transactivated with *Sa* RecA* (Figure 4C, Rum Mut-*Sa* + RecA* 4% PE). In accord with Rum Mut-*Ec*, the other Rum mutasomes were active, albeit weakly, with ATP (3–6% Figure 1E and Figure 4C). The specific activity for each Rum mutasome formed with ATPγS is given in Supplementary Table S1.

Relating Rum Mut DNA polymerase activities to Rum Pol spontaneous and DNA damage-induced mutation rates

We addressed the degree to which Rum Mut DNA synthesis measured biochemically (Figure 1E and 4C) correspond to mutation rates measured when Rum pol is introduced into *E. coli* expressing each of the seven RecA homologs. Rum pol is introduced either as a 'ready-to-go' post-translationally activated *rumA′B*, or as a *rumAB* operon encoded on the native R391 ICE (Figure 5).

To assess the full mutagenic potential of Rum pol uncoupled from its normal transcriptional and post-translational regulation, we first measured Rum pol-dependent spontaneous and MMS-induced mutagenesis using a *lexA51*(Def) *E. coli* strain in which all SOS regulated genes are constitutively expressed and also harbored chromosomal deletions of *umuDC* and *recA* genes (Δ*umuDC* Δ*recA*). The strain was transformed with two compatible low-copy-plasmids;

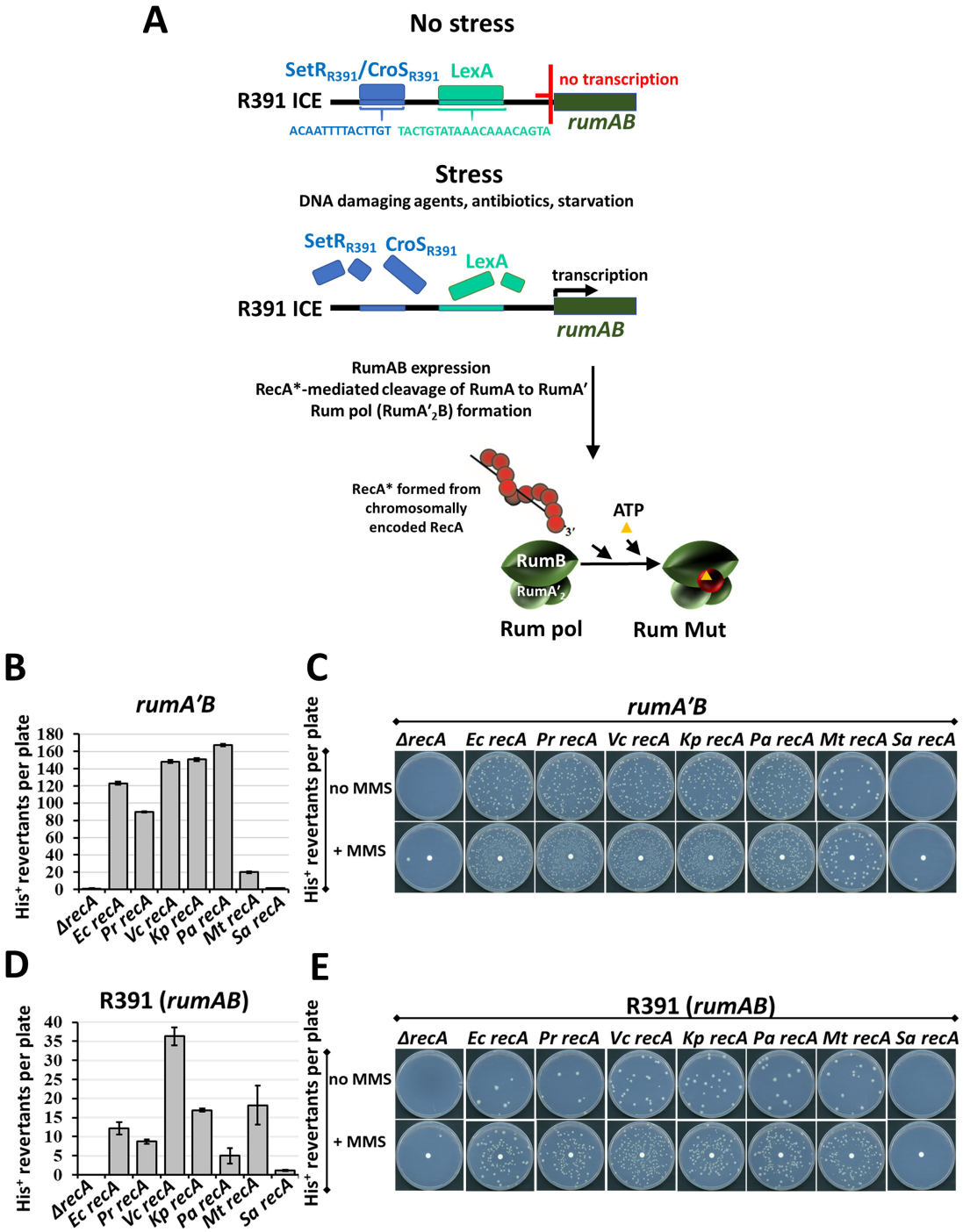

Figure 5. R391-encoded Rum pol requires RecA to be mutagenic. (**A**) Sketch depicting the three transcription repressors that control the expression of Rum pol from R391. LexA is encoded on the *E. coli* chromosome while SetR$_{R391}$ and CroS$_{R391}$ are encoded on R391. The repressors block *rumAB* transcription in the absence of DNA damage by binding to their respective consensus sequences in the promoter region of *rumAB* (40). SetR$_{R391}$ and CroS$_{R391}$ bind to the same consensus sequence meaning that only one of the proteins can bind to the site at any given time. The occurrence of cellular stress, e.g. by exposure to antibiotics and DNA damaging agents, causes cleavage and inactivation of LexA and SetR$_{R391}$, this allows for derepression of the *rumAB* operon before CroS$_{R391}$ can bind to the consensus site (40). Upon expression of the *rumAB* operon, RecA* facilitated autocatalytic cleavage of RumA to RumA′ results in the assembly of Rum pol (RumA′$_2$B), which is catalytically inactive. The catalytically active Rum Mut is formed by binding Rum pol to a RecA monomer encoded on the chromosome of the bacterial host, and the binding of an ATP molecule. (**B–E**) Rum pol spontaneous and MMS-induced mutagenesis was measured using a histidine reversion assay (reversion of *hisG4* ochre allele leading to histidine prototrophy [His$^+$]) in *E. coli* RW616 [*lexA51*(Def) *ΔumuC ΔrecA*] strain transformed with: (B, C) two low-copy plasmids, expressing *rumA′B* and *recA* genes; (D, E) or harboring the intact R391 ICE (expressing *rumAB*) and a low-copy plasmid encoding a RecA homolog. (B, D) Quantitative spontaneous mutagenesis rates presented as an average number of His$^+$ mutants from 15 individual plates per strain (± standard error of the mean [SEM]). (C, E) Qualitative MMS-induced mutagenesis. Representative plate images show Rum pol MMS-induced His$^+$ mutagenesis and its dependence on *recA*. Spontaneous and MMS-induced mutagenesis correlates with ability of Rum pol to form active complex with RecA (Figure 4).

one encoding a post-translationally activated RumA′B and second plasmid encoding *Ec* RecA, or a series of non-*Ec* RecA homologs expressed from the *Ec recA* promoter. Our data show that Rum spontaneous and MMS-induced mutagenesis are entirely *recA*-dependent (Figure 5B, C). No mutagenesis is observed in the complete absence of RecA, and we observed a 20–170-fold increase in the numbers of His^+ revertants per plate depending on the identity of the RecA homolog (Figure 5B). The largest increase in spontaneous mutagenesis (90–170-fold, Figure 5B) occurred for Rum mutasomes with the highest rates of p/t DNA extension (Figure 1E and 4C). Consistent with *in vitro* activity data (Figure 4C), Rum spontaneous mutagenesis was significantly reduced in a strain expressing *Mt* RecA and was abolished in a strain expressing *Sa* RecA (Figure 5B, C). A similar correlation between the biochemical and *in vivo* behavior of Rum pol was observed for induced mutagenesis using the DNA damaging agent methyl methane sulfonate (MMS) (Figure 5C).

Mutagenesis is dependent on the regulation of Rum pol

The expression of Rum pol from its natural R391 ICE is tightly regulated by the interplay of three transcriptional repressors (*Ec* LexA, $SetR_{R391}$ and $CroS_{R391}$) (37,40,60), as well as post-translationally by cleavage of RumA to RumA′ (37) (Figure 5A). Taking into consideration the highly complex mechanisms that govern the *in vivo* expression of *rumAB*, which subsequently require assembly of a mutasomal complex by binding Rum pol to RecA and ATP (Figure 1 and 4C), it is important to determine whether Rum pol is mutagenically active with a variety of RecA homologs, when expressed from its native R391 ICE.

We have measured spontaneous and MMS-induced mutagenesis in an *E. coli* strain [*lexA51*(Def) *ΔumuDC ΔrecA*] that is constitutively induced for SOS and harbors an intact R391 ICE encoding the *rumAB* operon, in the presence of low copy number plasmids carrying each of the RecA homologs (Figure 5D, E). The data showed similar RecA-dependent spontaneous and MMS-induced mutagenesis patterns that were observed for strains expressing post-translationally activated $RumA'_2B$ encoded on a low-copy number plasmid (Figure 5B, C). R391 Rum pol generated mutagenesis is RecA-dependent and correlates with ability of various RecAs to form active Rum Mut complexes (Figure 5D and 5E, compare with Figure 1 and 4C). The RecA homologs, except for *Sa* RecA, increase Rum pol mutagenesis. The strains expressing RumA′B show understandably higher His^+ mutation rates than those with RumAB encoded on R391 (compare Figure 5B, C with Figure 5D, E), which require additional regulatory steps (Figure 5A) including transcriptional derepression of the *rumAB* operon and the subsequent processing of RumA to RumA′ by RecA* mediated proteolysis. The pathogen encoded RecA's (with the exception of *Sa* RecA), were able to induce RumA cleavage *in vivo* upon exposure to the DNA damaging antibiotic Ciprofloxacin (Supplementary Figure S3 and Materials and Methods). Thus, the R391-dependent mutagenesis levels represent a composite of RecA-mediated regulatory processes used to regulate the expression of Rum pol for DNA synthesis, including cleavage of the LexA repressor protein, efficient RumA to RumA′ conversion required to form $RumA'_2B$ (Rum pol), and the subsequent assembly of active Rum Mut complexes. Our data demonstrate that the native R391-encoded Rum pol can be mutagenically activated by a variety of RecAs in potential host bacterial pathogens.

Notably, *E. coli* strains containing functional chromosomal copies of *umuDC, recA* and *lexA* genes together with R391 ICE showed 31% and 38% increases in spontaneous and MMS- induced mutagenesis (Supplementary Figure S4). This increased level of mutagenesis, albeit relatively small, indicates that a horizontally transferred MEPol forms an activated mutasomal complex. Transfer of the MEPol enhances the mutational diversity of host strains, while acting alongside chromosomally encoded homologs of pol V and is able to share the chromosomally expressed RecA.

Identification of a RecA amino-acid residue that fully restores mutagenesis of the barely active Rum Mut-*Mt*

A comparison of amino acid sequences of homologous RecAs able to form fully mutagenic Rum Mut with RecA that forms weakly active Rum Mut-*Mt* and inactive Rum Mut-*Sa* revealed amino acid differences that might be essential for Rum Mut-dependent mutagenesis (Figure 4A). Since Rum pol is weakly active with *Mt* RecA (Figure 4C and Figure 5B, C) we replaced several amino acids in *Mt* RecA with corresponding *Ec* RecA amino acids (Figure 4A) and determined the extent to which spontaneous mutagenesis has been altered in relation to Rum Mut-*Ec*. The His^+ mutagenesis was measured in *E. coli* strain transformed with two plasmids, one expressing $RumA'_2B$ and second plasmid expressing mutated *Mt* RecA variant (*Mt* RecA m1-m7). The seven *Mt* RecA mutated variants carry the following amino acid substitutions: *Mt* RecA m1: A76T, *Mt* RecA m2: A181 N, *Mt* RecA m3: T188 L, *Mt* RecA m4: D197M, *Mt* RecA m5: E230G T231A, *Mt* RecA m6: D261Q, *Mt* RecA m7: A33R R34S Q35M P36D. The *Ec* RecA mutant was constructed by replacing M197 with D, which is present at this position in *Mt* RecA. The replacement of a single amino acid (D197M) in *Mt* RecA m4 fully restored Rum pol mutagenesis; there was a 1.5-fold increase in His^+ reversion frequencies compared with *Ec* RecA (Figure 6). The remaining *Mt* RecA mutants either were not able to elevate Rum Mut-*Mt* mutagenesis to Rum Mut-*Ec* levels, or were mutagenically inactive possibly due to their inability to form activated Rum Mut complexes. Therefore, the replacement of a single amino acid in a host RecA resulted in a large increase in mutagenesis by converting poorly mutagenic Rum pol to fully mutagenic polymerase. The M197D mutation in *Ec* RecA decreases Rum pol-dependent mutagenesis to the level observed with *Mt* RecA further showing that this particular amino acid position is essential for Rum Mut mutagenic activity (Figure 6).

Until the structure of Rum Mut, or pol V Mut, is solved and interactions between subunits of the mutasome are precisely defined, it remains unclear how the M197 region of RecA impacts essential biochemical properties of Rum Mut, including complex formation, ability to bind ATP, and the DNA-dependent ATPase. It has been suggested that the

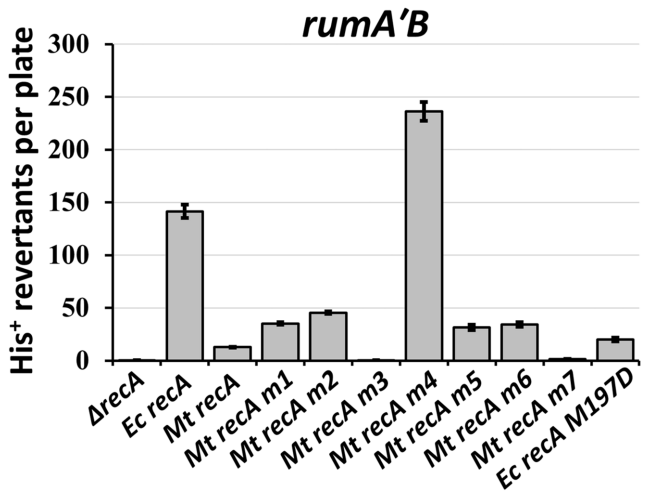

Figure 6. A single amino acid replacement in *Mt* RecA (D197M) converts the weakly mutagenic Rum Mut-*Mt* to a fully mutagenic mutasomal complex. Mutated variants of *Mt* RecA were constructed by replacing regions of weak homology in the *Mt* RecA (Figure 4A) with the corresponding amino acids in the *E. coli* RecA. Mutated variants of *Mt* RecA (*Mt* RecA m1-m7) were constructed by replacing *Mt* RecA amino acids with the corresponding amino acid in *Ec* RecA. The amino acid changes in *Mt* RecA m1-m7 mutants used are: *Mt* RecA m1: A76T, *Mt* RecA m2: A181 N, *Mt* RecA m3: T188 L, *Mt* RecA m4: D197M, *Mt* RecA m5: E230G T231A, *Mt* RecA m6: D261Q, *Mt* RecA m7: A33R R34S Q35M P36D. The *Ec* RecA mutant was constructed by replacing M197 with D, which is present at this position in *Mt* RecA. Spontaneous mutagenesis was measured using a histidine reversion assay in *E. coli* RW616 [*lexA51*(Def) *ΔumuC ΔrecA*] transformed with two low-copy plasmids, expressing *rumA′B* and *recA* homologs or expressing a mutated variant. The spontaneous mutagenesis rates are shown as the average number of His^+ revertants from 15 individual plates per strain (± standard error of the mean [SEM]).

L2 loop of RecA containing M197 might be essential for DNA binding and ATPase activity of multimeric RecA (61). Perhaps these functions also apply to Rum Mut and that the L2 loop of RecA may be involved in binding the mutasome to p/t DNA, and the D197M substitution in the *Mt* RecA m4 mutant restores the structural integrity of the RecA L2 loop. Future biochemical, and more importantly, structural studies of Rum Mut assembled with mutants of RecA in the L2 loop would likely lend considerable insight into how a single RecA monomer is able to exert such a strong impact on the properties of Rum Mut and its homologs both *in vitro* (Figure 4) and *in vivo* (Figure 5).

DISCUSSION

This study leads to four conclusions. First, like DNA polymerase V, the Rum family TLS polymerases require an acquired RecA subunit and ATP for activation. Activation generates Rum Mut, containing $RumA'_2B$-RecA-ATP (Figure 1). Second, Rum Mut can be generated using RecA proteins from a range of bacterial species, including many common pathogens (Figure 4). Third, the capacity of a cellular RecA to activate Rum pol *in vitro* and induce mutagenesis *in vivo* relates directly to the phylogenetic distance between RecA's of the major host(s) for an ICE (Figure 5). Fourth, a single amino acid change in a host RecA can convert a weakly mutagenic Rum Mut-*Mt* to fully mutagenic mutasomal complex (Figure 6).

In *E. coli*, DNA polymerase V plays a major role in mutagenesis. The *umuDC* homologs in pathogens likely make a similar contribution to mutagenesis, a contribution that can be strongly augmented by introduction of a mobile element encoding a Rum family polymerase. The resulting mutations can lead to antibiotic resistance, especially if the homologous pols copied DNA with unusually poor fidelity. Pol V carries out avid TLS *in vitro* (51) and copies undamaged DNA with extremely low fidelity *in vivo* in the range of 10^{-2} to 10^{-3} (62,63). When expressed in *E. coli,* Rum pol is ∼3- to 10-fold more mutagenic than pol V (37,39).

In this paper, we have investigated the pol V homolog, Rum Pol, and have explored the extent to which its biochemical regulatory properties are the same as *E. coli* pol V (31,51,58,64). A unique property of pol V is that it can only copy DNA when assembled as mutasomal complex, pol V Mut, containing a RecA monomer and a molecule of ATP (or ATPγS) (26,36). The same holds true for Rum pol. Rum pol, cannot copy p/t DNA by itself, but must be converted into an activated mutasomal complex via assembly with an *E. coli* RecA monomer and ATP, Rum Mut-*Ec* = $RumA'_2B$-*Ec* RecA–ATP (Figure 1C, E). A bound molecule of ATP/ATPγS as an integral component in the complex is required for Rum Mut to bind to p/t DNA (Figure 3; Supplementary Movie S1–S3). A 'unique' activity of pol V Mut is the presence of an intrinsic DNA-dependent ATPase. We have verified that this activity is retained in Rum Mut (Supplementary Figure S2). As observed for the *E. coli* and *V. cholerae* mutasomes, the DNA-dependent ATPase for Rum Mut requires the presence of RecA; the intrinsic ATPase remains active when bound to *Ec* RecA E38K/K72R, which contains a mutation in the Walker A motif that inactivates the canonical RecA-associated DNA-dependent ATPase (Supplementary Figure S2B). The biochemical and physiological significance of Rum Mut ATPase remains to be defined. Limited studies with pol V Mut showed that the ATPase catalyzed the release of the mutasome from p/t DNA (36,58). Both pol V Mut (36,51,58) and Rum Mut homologs (Figures 1, 2 and 4) are significantly more active when assembled with slowly-hydrolysable ATPγS compared to ATP. We speculate that perhaps ATP hydrolysis by Rum Mut and pol V Mut induce conformation changes that result in the reorientation of RecA on Rum pol and pol V that reduces mutasome affinity to DNA. An expedited dissociation from DNA could limit mutasome processivity and thereby limit mutagenesis to regions proximal to a bypassed lesion (33). How an intrinsic ATPase impacts the biological functions of the homologous Rum mutasomes remains to be studied, however it is clear that the intrinsic DNA-dependent ATPase adds an additional level of complexity to mechanisms that regulate the activity of this highly mutagenic polymerase.

Since Rum is encoded on a horizontally transmissible ICE, it would presumably need to partner with RecAs, specific to each of its host bacteria. Thus, the central finding of this paper is the ability of Rum Mut to assemble as an active polymerase by 'mixing and matching' RecA homologs purified from seven bacterial species (Figure 4). Rum Mut specific activities differ depending on the phylogenic distance of its RecA subunit from *Ec* RecA (Figure 4B), The activ-

ity of Rum Mut-*Pr* containing the phylogenetically close *Pr* RecA (Figure 4C) is essentially identical to Rum Mut-*Ec* (Figure 1E). Rum Mut shows decreased levels of activity as a function of diverging phylogenetic distance, culminating with an inactive Rum Mut-*Sa* (Figure 4C). However, although the Rum Mut-*Sa* has no detectible activity as a stand-alone mutasome, it is nevertheless able to copy DNA (albeit weakly) in the presence of transactivating *Sa* RecA* (Figure 4C, right-hand gel). Large increases in Rum pol spontaneous and MMS-induced mutagenesis occurred for the enzymatically active Rum mutasomes, whereas mutations were reduced significantly in *E. coli* expressing *Mt* RecA and were absent with *Sa* RecA (Figure 5). Importantly, a single amino acid change, D197M, converts the *Mt* RecA to a protein that fully activates Rum pol (Figure 6). Thus, even in a pathogen where an introduced ICE may not initially contribute to mutagenesis, a small genomic change can trigger a large increase in mutagenesis.

Gratuitous acquisition of a mutator phenotype would seldom, if ever, be beneficial to a recipient bacterial cell. The horizontal transfer of R391 DNA containing Rum pol into a recipient cell is unlikely to result in the expression of a hyper-mutator phenotype because of intervening levels of Rum pol regulation (20,40,60). The initial stage of regulation involves the presence of three transcriptional repressors (40,60). When transcription of *rumA* and *rumB* does occur, Rum pol can only be formed by the conversion RumA to RumA′ via RecA*-mediated proteolysis (37). RumA′ is needed for the assembly of Rum pol (37). In *E. coli*, the assembly of Rum pol requires the induction of the SOS response. The presence of antibiotics, even those that do not interact directly with DNA, have been observed to induce SOS in *E. coli* (14,18). The conversion of inactive Rum pol (RumA′$_2$B) into activated Rum Mut (Rum A′$_2$B-RecA-ATP) (Figure 1) can be viewed as the tip of a regulatory hierarchy, a final necessary step to generate a mutator phenotype in recipient cells, which would in principle provide a way for cells to develop tolerance and resistance to drugs.

Bacteria growing in the wild suffer almost constant environmental hazards where lengthy periods of stress, including nutrient deprivation and exposure to genotoxic chemicals, tend to be the rule rather than the exception. Mobile elements, including ICEs contribute to genome plasticity and acquisition of novel traits by the host, such as antibiotic resistance and alterations in cellular metabolism (65,66). Whether having an R391 ICE has beneficial, or detrimental, effects on a host cell will likely depend on the selective forces exerting effects on both the mobile element and on the host chromosome. R391-encoded Rum pol is an especially powerful mutator, having a mutation frequency 3- to 10-fold greater than *E. coli* pol V (19,37,39,40). However, potential detrimental effects and metabolic burdens of Rum pol mutagenesis are likely negligible in the absence of environmental stress, owing to the stringent repression of Rum pol expression by proteins encoded by both the R391 ICE (SetR$_{R391}$ and CroS$_{R391}$ repressors) and the host chromosome (LexA and RecA) (40,60). Through its SOS response to DNA damage, the host cell determines exactly when and under what conditions to produce Rum pol, and then to allow it to synthesize DNA by donating a host cell encoded RecA monomer. How Rum pol might influence the rate of adaptive evolution is not yet known.

There remain many gaps in knowledge that remain to be filled prior to demonstrating a role of for PEPols and mobile MEPols as an essential source of mutations leading to drug tolerance and drug resistance (67–69). Rum pol can be assembled into an active mutasome by binding RecA monomers from a wide variety of bacteria, with its biochemical and mutagenic activities linked to the phylogenetic distance of the RecAs from *E. coli* RecA. If conserved in other MEPols, the ability to assemble a mutasome using a recipient cell's RecA could provide a general mechanism to account for the mutation-driven evolution of bacterial pathogens and a possible mechanism of acquisition of multidrug resistance.

DATA AVAILABILITY

Source data as well as plasmids and strains are available upon request.

SUPPLEMENTARY DATA

Supplementary Data are available at NAR Online.

ACKNOWLEDGEMENTS

We thank Dr. Len Adelman for his insightful and constructive comments.

FUNDING

National Institute of Environmental Health Sciences [R35ES028343 to M.F.G.]; National Institutes of General Medical Sciences [1RM1GM130450 to M.F.G., M.M.C., A.R. and A.V.]; National Institutes of Child Health and Human Development, National Institutes of Health [Intramural Research Program to R.W.]; National Institute of Neurological Disorders and Stroke, National Institutes of Health [R21NS114911 to F.P.]; National Science Foundation [CHE-1664801 to C.M.]. Funding for open access charge: National Institutes of General Medical Sciences [1RM1GM130450].

Conflict of interest statement. None declared.

REFERENCES

1. Rodriguez-Beltran,J., DelaFuente,J., Leon-Sampedro,R., MacLean,R.C. and San Millan,A. (2021) Beyond horizontal gene transfer: the role of plasmids in bacterial evolution. *Nat. Rev. Microbiol.*, **19**, 347–359.
2. Peterson,E. and Kaur,P. (2018) Antibiotic resistance mechanisms in bacteria: relationships between resistance determinants of antibiotic producers, environmental bacteria, and clinical pathogens. *Front. Microbiol.*, **9**, 2928.
3. Alekshun,M.N. and Levy,S.B. (2007) Molecular mechanisms of antibacterial multidrug resistance. *Cell*, **128**, 1037–1050.
4. Merrikh,H. and Kohli,R.M. (2020) Targeting evolution to inhibit antibiotic resistance. *FEBS J.*, **287**, 4341–4353.
5. Botelho,J. and Schulenburg,H. (2021) The role of integrative and conjugative elements in antibiotic resistance evolution. *Trends Microbiol.*, **29**, 8–18.
6. Barrett,T.C., Mok,W.W.K., Murawski,A.M. and Brynildsen,M.P. (2019) Enhanced antibiotic resistance development from fluoroquinolone persisters after a single exposure to antibiotic. *Nat. Commun.*, **10**, 1177.

7. Mo,C.Y., Manning,S.A., Roggiani,M., Culyba,M.J., Samuels,A.N., Sniegowski,P.D., Goulian,M. and Kohli,R.M. (2016) Systematically altering bacterial SOS activity under stress reveals therapeutic strategies for potentiating antibiotics. *mSphere*, **1**, e00163-16.
8. Revitt-Mills,S.A. and Robinson,A. (2020) Antibiotic-induced mutagenesis: under the microscope. *Front Microbiol*, **11**, 585175.
9. Ragheb,M.N., Thomason,M.K., Hsu,C., Nugent,P., Gage,J., Samadpour,A.N., Kariisa,A., Merrikh,C.N., Miller,S.I., Sherman,D.R. *et al.* (2019) Inhibiting the evolution of antibiotic resistance. *Mol. Cell*, **73**, 157–165.
10. Long,H., Miller,S.F., Strauss,C., Zhao,C., Cheng,L., Ye,Z., Griffin,K., Te,R., Lee,H., Chen,C.C. *et al.* (2016) Antibiotic treatment enhances the genome-wide mutation rate of target cells. *Proc. Natl. Acad. Sci. U.S.A.*, **113**, E2498–E2505.
11. Handel,N., Hoeksema,M., Freijo Mata,M., Brul,S. and ter Kuile,B.H. (2015) Effects of stress, reactive oxygen species, and the SOS response on *de novo* acquisition of antibiotic resistance in *escherichiacoli*. *Antimicrob. Agents Chemother.*, **60**, 1319–1327.
12. Pribis,J.P., Garcia-Villada,L., Zhai,Y., Lewin-Epstein,O., Wang,A.Z., Liu,J., Xia,J., Mei,Q., Fitzgerald,D.M., Bos,J. *et al.* (2019) Gamblers: an antibiotic-induced evolvable cell subpopulation differentiated by reactive-oxygen-induced general stress response. *Mol. Cell*, **74**, 785–800.
13. Bernier,S.P., Lebeaux,D., DeFrancesco,A.S., Valomon,A., Soubigou,G., Coppee,J.Y., Ghigo,J.M. and Beloin,C. (2013) Starvation, together with the SOS response, mediates high biofilm-specific tolerance to the fluoroquinolone ofloxacin. *PLoS Genet.*, **9**, e1003144.
14. Miller,C., Thomsen,L.E., Gaggero,C., Mosseri,R., Ingmer,H. and Cohen,S.N. (2004) SOS response induction by β-lactams and bacterial defense against antibiotic lethality. *Science*, **305**, 1629–1631.
15. Norton,M.D., Spilkia,A.J. and Godoy,V.G. (2013) Antibiotic resistance acquired through a DNA damage-inducible response in *Acinetobacter baumannii*. *J. Bacteriol.*, **195**, 1335–1345.
16. Crane,J.K., Alvarado,C.L. and Sutton,M.D. (2021) Role of the SOS response in the generation of antibiotic resistance *in vivo*. *Antimicrob. Agents Chemother.*, **65**, e0001321.
17. Cirz,R.T., Chin,J.K., Andes,D.R., de Crecy-Lagard,V., Craig,W.A. and Romesberg,F.E. (2005) Inhibition of mutation and combating the evolution of antibiotic resistance. *PLoS Biol.*, **3**, e176.
18. Kohanski,M.A., Dwyer,D.J., Hayete,B., Lawrence,C.A. and Collins,J.J. (2007) A common mechanism of cellular death induced by bactericidal antibiotics. *Cell*, **130**, 797–810.
19. Ho,C., Kulaeva,O.I., Levine,A.S. and Woodgate,R. (1993) A rapid method for cloning mutagenic DNA repair genes: isolation of *umu*-complementing genes from multidrug resistance plasmids R391, R446b, and R471a. *J. Bacteriol.*, **175**, 5411–5419.
20. Pinney,R.J. (1980) Distribution among incompatibility groups of plasmids that confer UV mutability and UV resistance. *Mutat. Res.*, **72**, 155–159.
21. Ryan,M.P., Slattery,S. and Pembroke,J.T. (2019) A novel arsenate-resistant determinant associated with ICEpMERPH, a member of the SXT/R391 group of mobile genetic elements. *Genes (Basel)*, **10**, 1048.
22. Slattery,S., Tony Pembroke,J., Murnane,J.G. and Ryan,M.P. (2020) Isolation, nucleotide sequencing and genomic comparison of a novel SXT/R391 ICE mobile genetic element isolated from a municipal wastewater environment. *Sci. Rep.*, **10**, 8716.
23. Williams,K.P., Gillespie,J.J., Sobral,B.W., Nordberg,E.K., Snyder,E.E., Shallom,J.M. and Dickerman,A.W. (2010) Phylogeny of gammaproteobacteria. *J. Bacteriol.*, **192**, 2305–2314.
24. Reuven,N.B., Arad,G., Maor-Shoshani,A. and Livneh,Z. (1999) The mutagenesis protein UmuC is a DNA polymerase activated by UmuD′, RecA, and SSB and is specialized for translesion replication. *J. Biol. Chem.*, **274**, 31763–31766.
25. Robinson,A., McDonald,J.P., Caldas,V.E., Patel,M., Wood,E.A., Punter,C.M., Ghodke,H., Cox,M.M., Woodgate,R., Goodman,M.F. *et al.* (2015) Regulation of mutagenic DNA polymerase V activation in space and time. *PLoS Genet.*, **11**, e1005482.
26. Jiang,Q., Karata,K., Woodgate,R., Cox,M.M. and Goodman,M.F. (2009) The active form of DNA polymerase V is UmuD′$_2$C-RecA-ATP. *Nature*, **460**, 359–363.
27. Pham,P., Seitz,E.M., Saveliev,S., Shen,X., Woodgate,R., Cox,M.M. and Goodman,M.F. (2002) Two distinct modes of RecA action are required for DNA polymerase V-catalyzed translesion synthesis. *Proc. Natl. Acad. Sci. U.S.A.*, **99**, 11061–11066.
28. Schlacher,K., Cox,M.M., Woodgate,R. and Goodman,M.F. (2006) RecA acts in *trans* to allow replication of damaged DNA by DNA polymerase V. *Nature*, **442**, 883–887.
29. Schlacher,K., Leslie,K., Wyman,C., Woodgate,R., Cox,M.M. and Goodman,M.F. (2005) DNA polymerase V and RecA protein, a minimal mutasome. *Mol. Cell*, **17**, 561–572.
30. Tang,M., Shen,X., Frank,E.G., O'Donnell,M., Woodgate,R. and Goodman,M.F. (1999) UmuD′$_2$C is an error-prone DNA polymerase, *Escherichia coli* pol V. *Proc. Natl. Acad. Sci. U.S.A.*, **96**, 8919–8924.
31. Jaszczur,M., Bertram,J.G., Robinson,A., van Oijen,A.M., Woodgate,R., Cox,M.M. and Goodman,M.F. (2016) Mutations for worse or better: low-fidelity DNA synthesis by SOS DNA polymerase V is a tightly regulated double-edged sword. *Biochemistry*, **55**, 2309–2318.
32. Gruber,A.J., Erdem,A.L., Sabat,G., Karata,K., Jaszczur,M.M., Vo,D.D., Olsen,T.M., Woodgate,R., Goodman,M.F. and Cox,M.M. (2015) A RecA protein surface required for activation of DNA polymerase V. *PLoS Genet.*, **11**, e1005066.
33. Isogawa,A., Ong,J.L., Potapov,V., Fuchs,R.P. and Fujii,S. (2018) Pol V-mediated translesion synthesis elicits localized untargeted mutagenesis during post-replicative gap repair. *Cell Rep.*, **24**, 1290–1300.
34. Karata,K., Vaisman,A., Goodman,M.F. and Woodgate,R. (2012) Simple and efficient purification of *Escherichia coli* DNA polymerase V: cofactor requirements for optimal activity and processivity *in vitro*. *DNA Repair (Amst.)*, **11**, 431–440.
35. Tang,M., Bruck,I., Eritja,R., Turner,J., Frank,E.G., Woodgate,R., O'Donnell,M. and Goodman,M.F. (1998) Biochemical basis of SOS-induced mutagenesis in *Escherichia coli*: reconstitution of *in vitro* lesion bypass dependent on the UmuD′$_2$C mutagenic complex and RecA protein. *Proc. Natl. Acad. Sci. U.S.A.*, **95**, 9755–9760.
36. Erdem,A.L., Jaszczur,M., Bertram,J.G., Woodgate,R., Cox,M.M. and Goodman,M.F. (2014) DNA polymerase V activity is autoregulated by a novel intrinsic DNA-dependent ATPase. *Elife*, **3**, e02384.
37. Kulaeva,O.I., Wootton,J.C., Levine,A.S. and Woodgate,R. (1995) Characterization of the *umu*-complementing operon from R391. *J. Bacteriol.*, **177**, 2737–2743.
38. Dutreix,M., Moreau,P.L., Bailone,A., Galibert,F., Battista,J.R., Walker,G.C. and Devoret,R. (1989) New *recA* mutations that dissociate the various RecA protein activities in *Escherichia coli* provide evidence for an additional role for RecA protein in UV mutagenesis. *J. Bacteriol.*, **171**, 2415–2423.
39. Mead,S., Vaisman,A., Valjavec-Gratian,M., Karata,K., Vandewiele,D. and Woodgate,R. (2007) Characterization of pol V_{R391}: a Y-family polymerase encoded by *rumA′B* from the IncJ conjugative transposon, R391. *Mol. Microbiol.*, **63**, 797–810.
40. McDonald,J.P., Quiros,D.R., Vaisman,A., Mendez,A.R., Reyelt,J., Schmidt,M., Gonzalez,M. and Woodgate,R. (2021) $CroS_{R391}$, an ortholog of the λ cro repressor, plays a major role in suppressing pol V_{R391} -dependent mutagenesis. *Mol. Microbiol.*, **116**, 877–889.
41. Szekeres,E.S. Jr, Woodgate,R. and Lawrence,C.W. (1996) Substitution of *mucAB* or *rumAB* for *umuDC* alters the relative frequencies of the two classes of mutations induced by a site-specific T-T cyclobutane dimer and the efficiency of translesion DNA synthesis. *J. Bacteriol.*, **178**, 2559–2563.
42. Burrus,V., Marrero,J. and Waldor,M.K. (2006) The current ICE age: biology and evolution of SXT-related integrating conjugative elements. *Plasmid*, **55**, 173–183.
43. Uhlin,B.E., Volkert,M.R., Clark,A.J., Sancar,A. and Rupp,W.D. (1982) Nucleotide sequence of a *recA* operator mutation. LexA/operator-repressor binding/inducible repair. *Mol. Gen. Genet.*, **185**, 251–254.
44. Cox,M.M., McEntee,K. and Lehman,I.R. (1981) A simple and rapid procedure for the large scale purification of the RecA protein of *Escherichiacoli*. *J. Biol. Chem.*, **256**, 4676–4678.
45. Lusetti,S.L., Wood,E.A., Fleming,C.D., Modica,M.J., Korth,J., Abbott,L., Dwyer,D.W., Roca,A.I., Inman,R.B. and Cox,M.M. (2003) C-terminal deletions of the *Escherichia coli* RecA protein. Characterization of *in vivo* and *in vitro* effects. *J. Biol. Chem.*, **278**, 16372–16380.

46. Lovett,S.T. and Kolodner,R.D. (1989) Identification and purification of a single-stranded-DNA-specific exonuclease encoded by the *recJ* gene of *Escherichia coli*. *Proc. Natl. Acad. Sci. U.S.A.*, **86**, 2627–2631.
47. Chin,J.W., Santoro,S.W., Martin,A.B., King,D.S., Wang,L. and Schultz,P.G. (2002) Addition of *p*-azido-L-phenylalanine to the genetic code of *Escherichia coli*. *J. Am. Chem. Soc.*, **124**, 9026–9027.
48. Young,T.S., Ahmad,I., Yin,J.A. and Schultz,P.G. (2010) An enhanced system for unnatural amino acid mutagenesis in *E. coli*. *J. Mol. Biol.*, **395**, 361–374.
49. Sambrook,J., Fritsch,E.F. and Maniatis,T. (1989) In: *Molecular Cloning: A Laboratory Manual*. Cold Spring Harbor Laboratory, NY.
50. Davis,B.D. and Mingioli,E.S. (1950) Mutants of *Escherichia coli* requiring methionine or vitamin B12. *J. Bacteriol.*, **60**, 17–28.
51. Sikand,A., Jaszczur,M., Bloom,L.B., Woodgate,R., Cox,M.M. and Goodman,M.F. (2021) The SOS error-prone DNA polymerase V mutasome and β-sliding clamp acting in concert on undamaged DNA and during translesion synthesis. *Cells*, **10**, 1083.
52. Chandradoss,S.D., Haagsma,A.C., Lee,Y.K., Hwang,J.H., Nam,J.M. and Joo,C. (2014) Surface passivation for single-molecule protein studies. *J. Vis. Exp.***86**, 50549.
53. Aitken,C.E., Marshall,R.A. and Puglisi,J.D. (2008) An oxygen scavenging system for improvement of dye stability in single-molecule fluorescence experiments. *Biophys. J.*, **94**, 1826–1835.
54. Brune,M., Hunter,J.L., Corrie,J.E. and Webb,M.R. (1994) Direct, real-time measurement of rapid inorganic phosphate release using a novel fluorescent probe and its application to actomyosin subfragment 1 ATPase. *Biochemistry*, **33**, 8262–8271.
55. Brune,M., Hunter,J.L., Howell,S.A., Martin,S.R., Hazlett,T.L., Corrie,J.E. and Webb,M.R. (1998) Mechanism of inorganic phosphate interaction with phosphate binding protein from *Escherichia coli*. *Biochemistry*, **37**, 10370–10380.
56. Di Capua,E., Engel,A., Stasiak,A. and Koller,T. (1982) Characterization of complexes between RecA protein and duplex DNA by electron microscopy. *J. Mol. Biol.*, **157**, 87–103.
57. Dombroski,D.F., Scraba,D.G., Bradley,R.D. and Morgan,A.R. (1983) Studies of the interaction of RecA protein with DNA. *Nucleic Acids Res.*, **11**, 7487–7504.
58. Jaszczur,M.M., Vo,D.D., Stanciauskas,R., Bertram,J.G., Sikand,A., Cox,M.M., Woodgate,R., Mak,C.H., Pinaud,F. and Goodman,M.F. (2019) Conformational regulation of *Escherichia coli* DNA polymerase V by RecA and ATP. *PLoS Genet.*, **15**, e1007956.
59. Gruenig,M.C., Renzette,N., Long,E., Chitteni-Pattu,S., Inman,R.B., Cox,M.M. and Sandler,S.J. (2008) RecA-mediated SOS induction requires an extended filament conformation but no ATP hydrolysis. *Mol. Microbiol.*, **69**, 1165–1179.
60. Gonzalez,M., Huston,D., McLenigan,M.P., McDonald,J.P., Garcia,A.M., Borden,K.S. and Woodgate,R. (2019) $SetR_{ICE391}$, a negative transcriptional regulator of the integrating conjugative element R391 mutagenic response. *DNA Repair (Amst.)*, **73**, 99–109.
61. Hortnagel,K., Voloshin,O.N., Kinal,H.H., Ma,N., Schaffer-Judge,C. and Camerini-Otero,R.D. (1999) Saturation mutagenesis of the *E. coli* RecA loop L2 homologous DNA pairing region reveals residues essential for recombination and recombinational repair. *J. Mol. Biol.*, **286**, 1097–1106.
62. Sweasy,J.B., Witkin,E.M., Sinha,N. and Roegner-Maniscalco,V. (1990) RecA protein of *Escherichia coli* has a third essential role in SOS mutator activity. *J. Bacteriol.*, **172**, 3030–3036.
63. Fijalkowska,I.J., Dunn,R.L. and Schaaper,R.M. (1997) Genetic requirements and mutational specificity of the *Escherichia coli* SOS mutator activity. *J. Bacteriol.*, **179**, 7435–7445.
64. Goodman,M.F., McDonald,J.P., Jaszczur,M.M. and Woodgate,R. (2016) Insights into the complex levels of regulation imposed on *Escherichia coli* DNA polymerase V. *DNA Repair (Amst.)*, **44**, 42–50.
65. Johnson,C.M. and Grossman,A.D. (2015) Integrative and conjugative elements (ICEs): what they do and how they work. *Annu. Rev. Genet.*, **49**, 577–601.
66. Wozniak,R.A. and Waldor,M.K. (2010) Integrative and conjugative elements: mosaic mobile genetic elements enabling dynamic lateral gene flow. *Nat. Rev. Microbiol.*, **8**, 552–563.
67. Liu,J., Gefen,O., Ronin,I., Bar-Meir,M. and Balaban,N.Q. (2020) Effect of tolerance on the evolution of antibiotic resistance under drug combinations. *Science*, **367**, 200–204.
68. Levin-Reisman,I., Ronin,I., Gefen,O., Braniss,I., Shoresh,N. and Balaban,N.Q. (2017) Antibiotic tolerance facilitates the evolution of resistance. *Science*, **355**, 826–830.
69. Levin-Reisman,I., Brauner,A., Ronin,I. and Balaban,N.Q. (2019) Epistasis between antibiotic tolerance, persistence, and resistance mutations. *Proc. Natl. Acad. Sci. U.S.A.*, **116**, 14734–14739.
70. Churchward,G., Belin,D. and Nagamine,Y. (1984) A pSC101-derived plasmid which shows no sequence homology to other commonly used cloning vectors. *Gene*, **31**, 165–171.
71. Ghodke,H., Paudel,B.P., Lewis,J.S., Jergic,S., Gopal,K., Romero,Z.J., Wood,E.A., Woodgate,R., Cox,M.M. and van Oijen,A.M. (2019) Spatial and temporal organization of RecA in the *Escherichia coli* DNA-damage response. *Elife*, **8**, e42761.